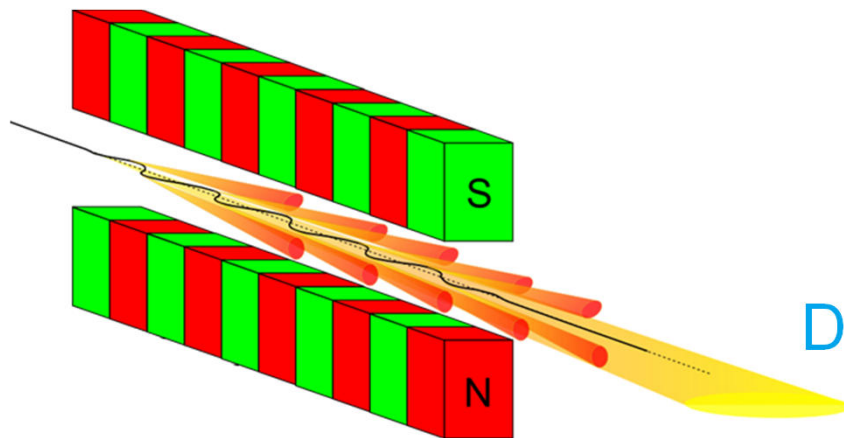


Numerical Modeling of Collective Effects in Free Electron Laser

Mathematical Model and Numerical Algorithms



Igor Zagorodnov

Deutsches Elektronen Synchrotron,
Hamburg, Germany

ICAP 2012, Rostock
21. August 2012

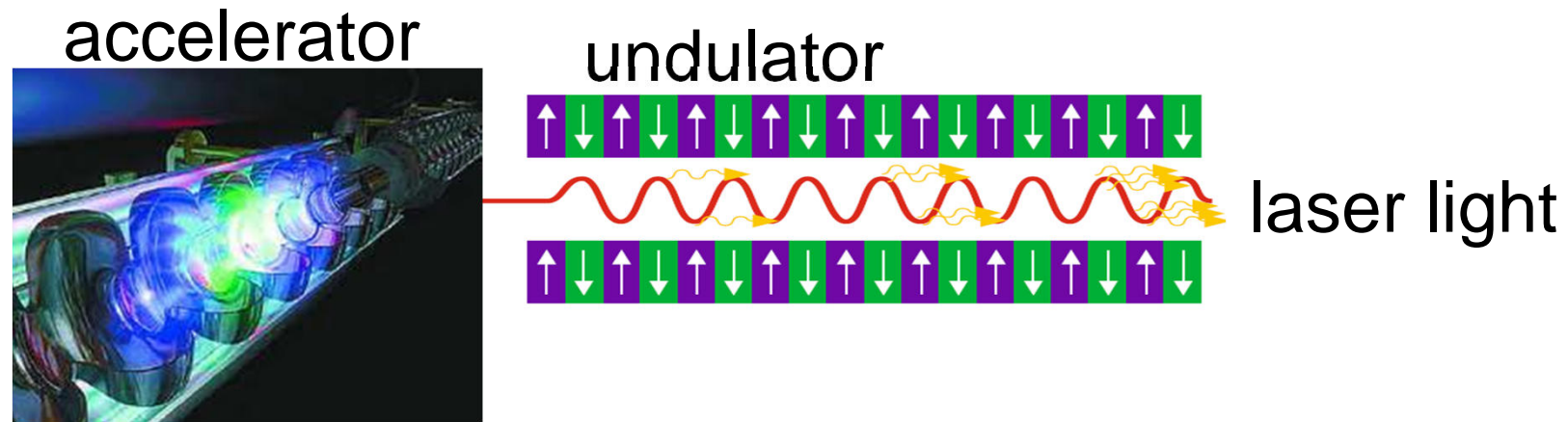
Overview

- ❑ motivation
- ❑ FEL physics in 1D
- ❑ mathematical model in 3D
- ❑ numerical methods
- ❑ quiet start and shot noise
- ❑ time dependent simulations
- ❑ problems and challenges



Motivation

Free Electron Laser



- ❑ very short and tunable wavelength
- ❑ extreme short pulses with very high energy

John Madey, Appl. Phys. **42**, 1906 (1971)

Motivation

FLASH („Free Electron LASer in Hamburg“)

gun



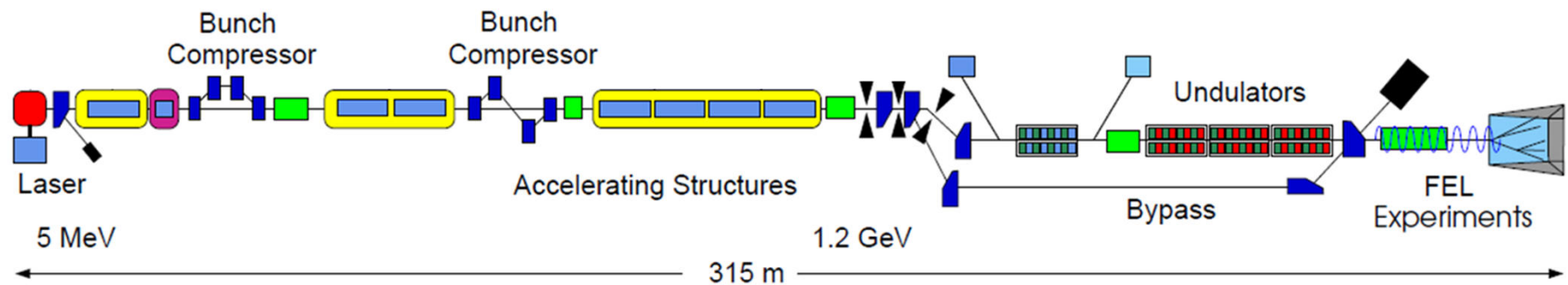
accelerator



undulator



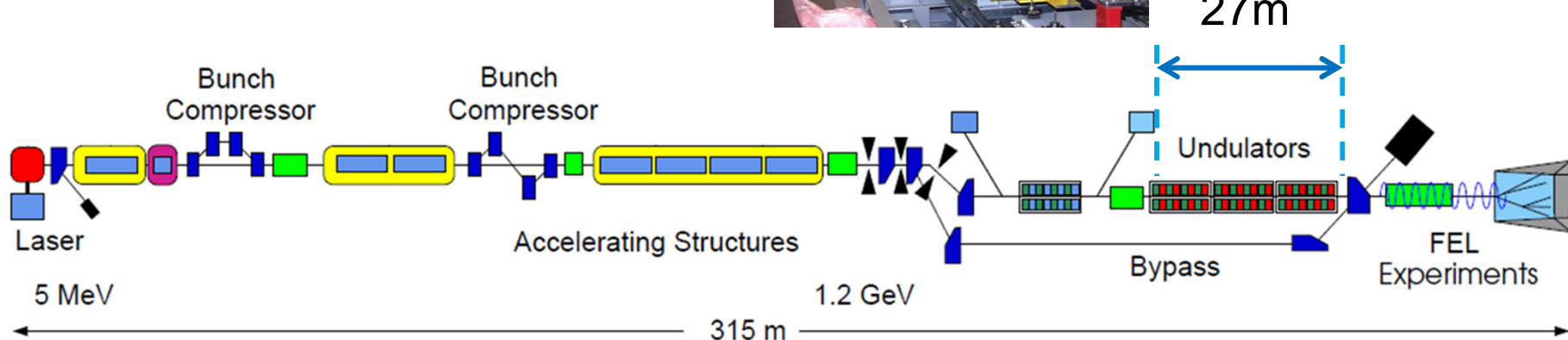
laboratory



Motivation

FLASH („Free Electron LASer in Hamburg)

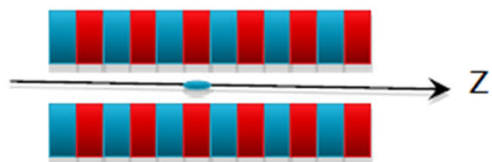
undulator



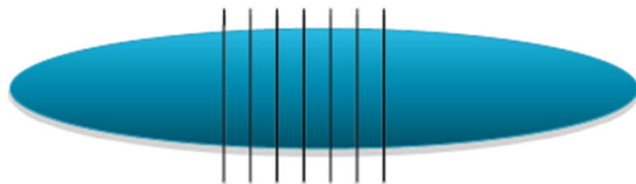
Motivation

Numerical methods

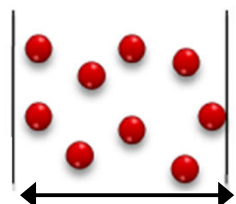
- ▶ undulator (~ 100 m)



- ▶ bunch ($\sim 10 \mu\text{m}$)



- ▶ slice ($\sim 0.1 \text{ nm}$)



λ – Wellenlänge

S. Reiche, *FEL simulations: history, status and outlook*, FEL 2010, Malmö, 2010



12 orders of magnitude



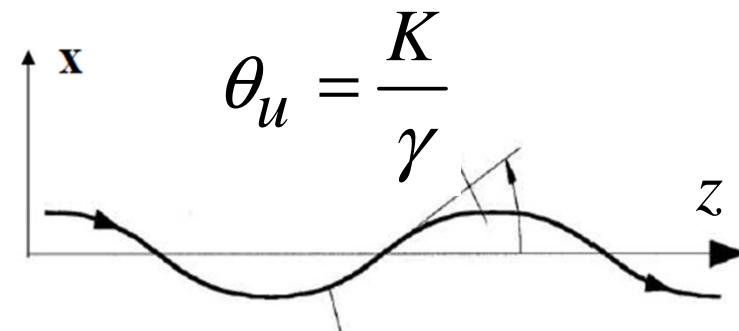
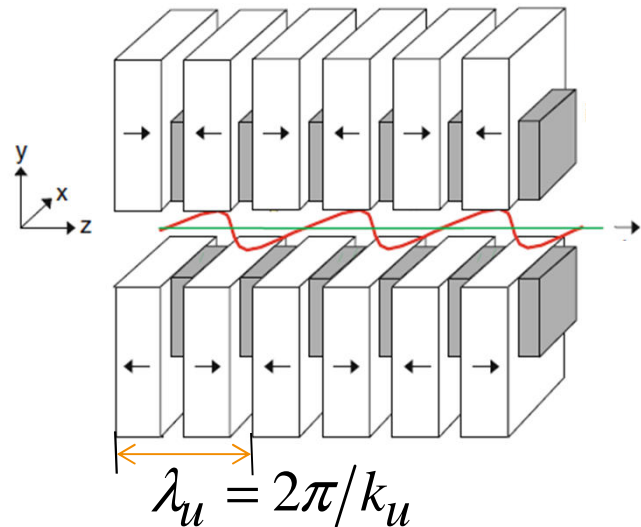
approximations
are necessary



FEL numerical
algorithms

FEL Physics in 1D

Motion of one electron in an undulator



electron trajectory

Field on the axis

$$B_y = -B_0 \sin(k_u z)$$

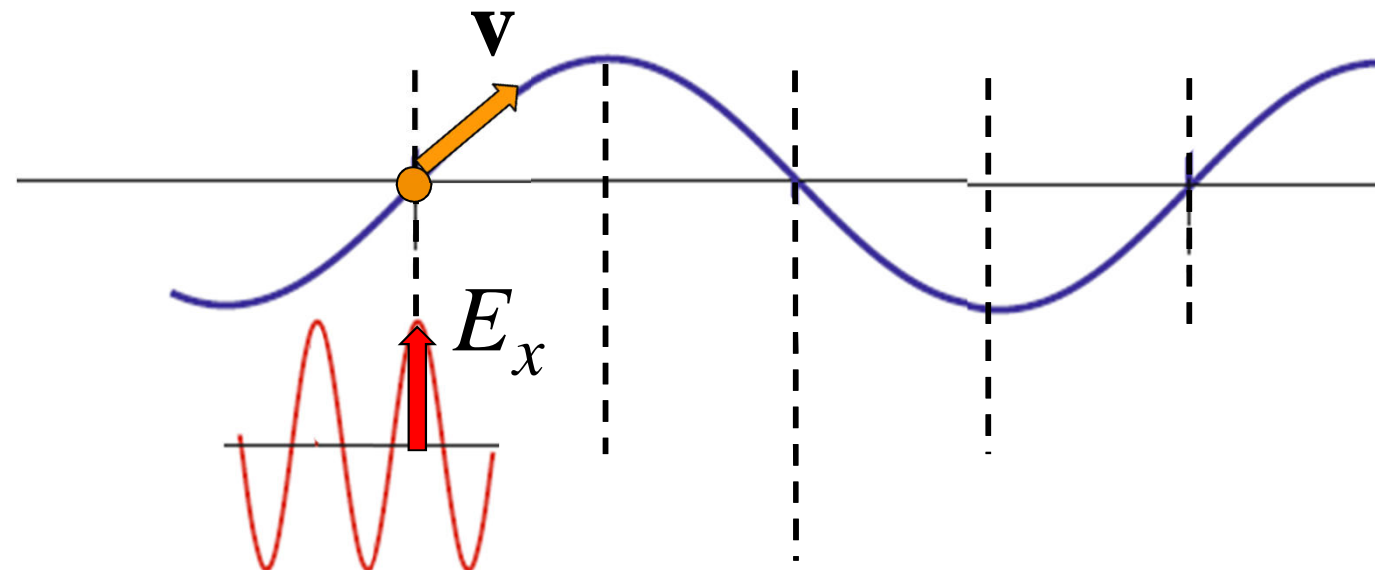
$$K = \frac{eB_0}{m_e c k_u} \text{ - undulator parameter}$$

γ - electron energy

FEL Physics in 1D

Energy exchange in FEL

$\bar{v}_z < c$ an electron is slower than the EM field



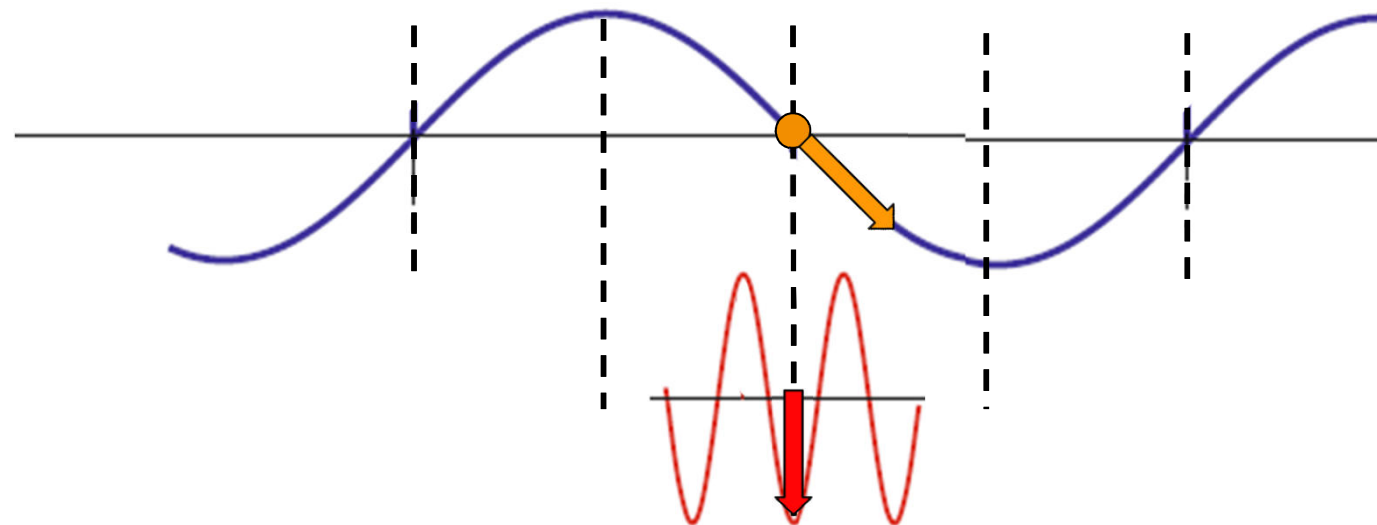
EM field \sim plane wave

$$E_x(z, t) = E_0 \cos(kz - \omega t)$$

FEL Physics in 1D

Energy exchange in FEL

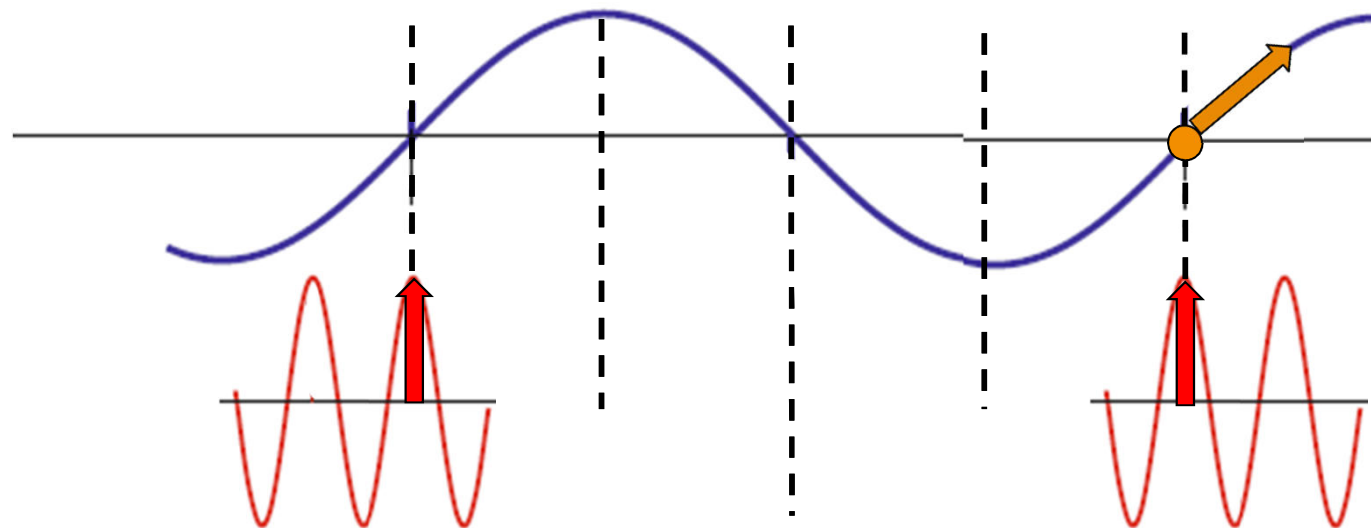
$\bar{v}_z < c$ an electron is slower than the EM field



FEL Physics in 1D

Energy exchange in FEL

$\bar{v}_z < c$ an electron is slower than the EM field



The electron has to be slower exactly by one wave length.

$$\lambda = \frac{\lambda_u}{2\gamma^2} \left(1 + \frac{K^2}{2} \right)$$

FEL Physics in 1D

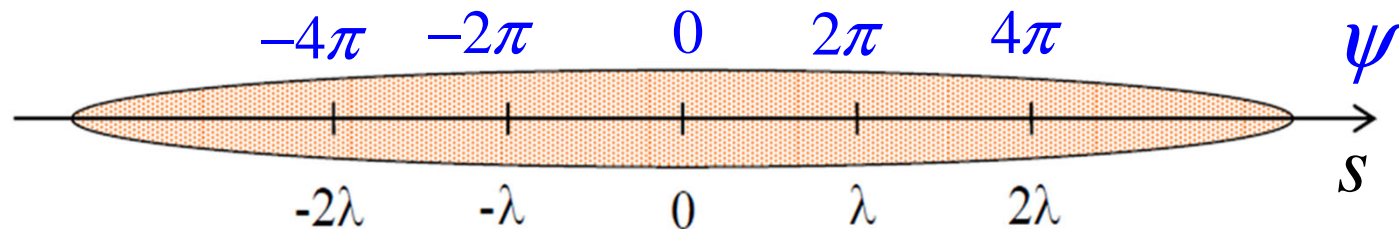
Longitudinal equations of motion (1D model)

$$\frac{d}{dt}\psi = 2k_u c \eta$$

$$\frac{d}{dt}\eta = -\frac{eK[JJ]E_0}{2m_e c \gamma_r^2} \cos \psi$$

$$\psi = (k + k_u)z - \omega t, [JJ] \sim 1$$

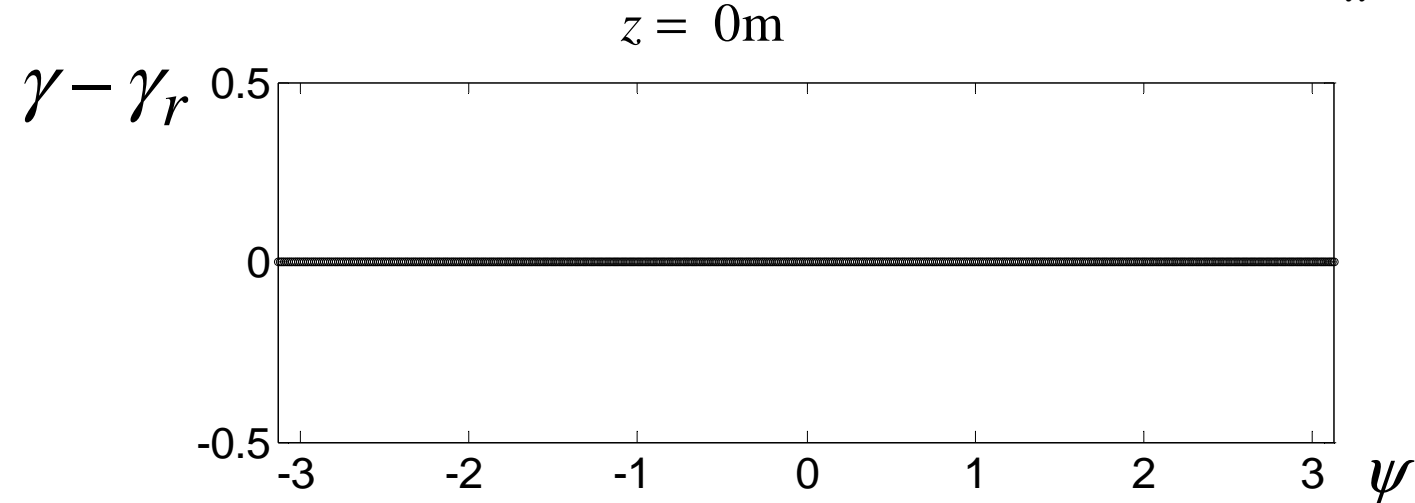
$$\eta = \frac{\gamma - \gamma_r}{\gamma_r}$$



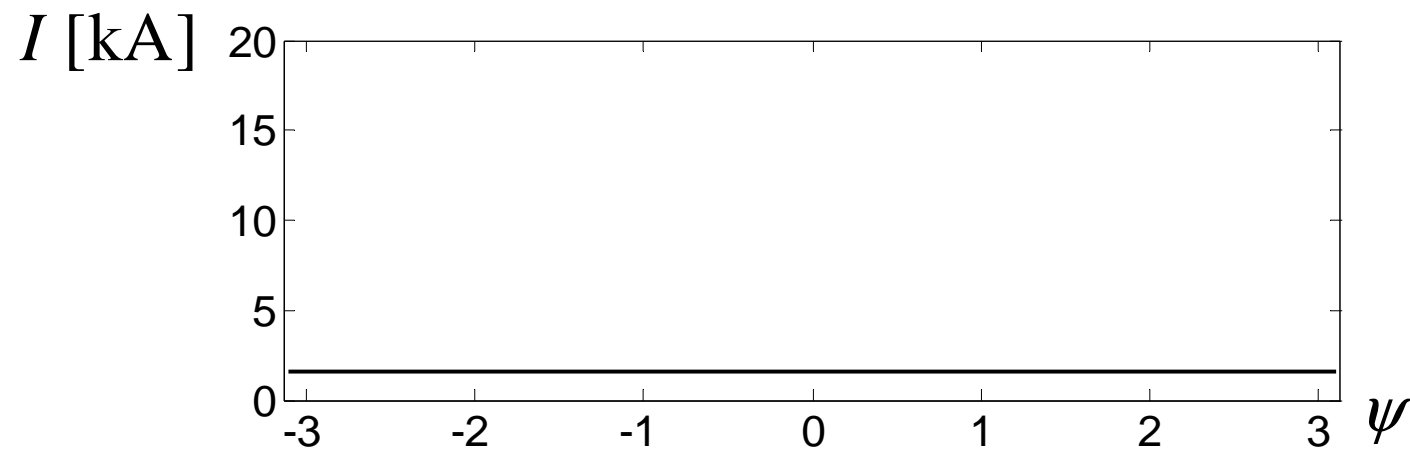
FEL Physics in 1D

„Low gain“ FEL

$$E_x(0) = 30 \text{ MV/m}$$



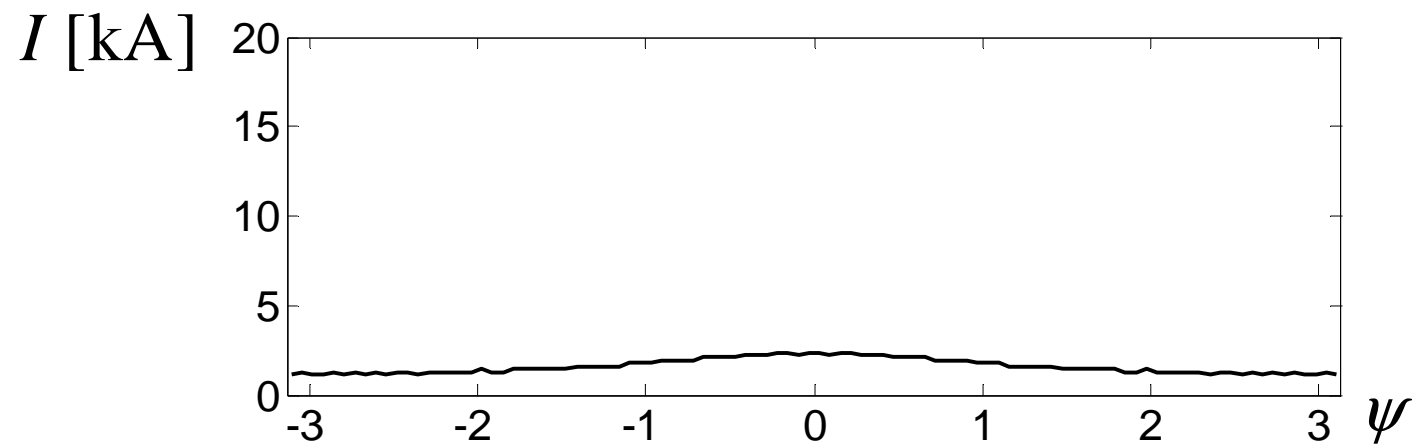
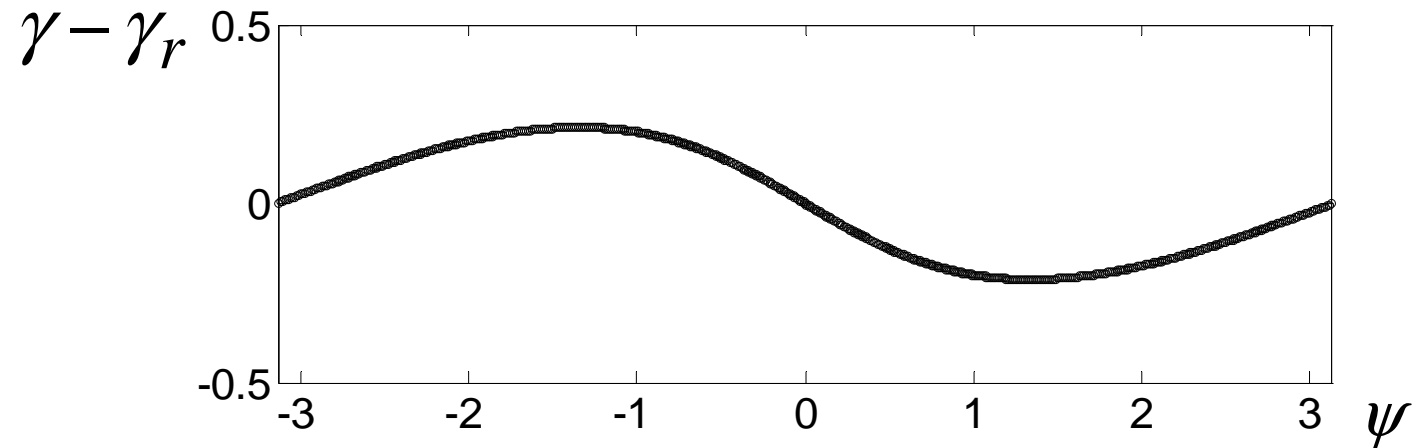
$$\begin{aligned} r_{beam} &= 0.1 \text{ mm} \\ \lambda_u &= 27 \text{ mm} \\ K &= 1.2 \\ \lambda &= 6 \text{ nm} \\ I_{peak} &= 1.6 \text{ kA} \end{aligned}$$



FEL Physics in 1D

„Low gain“ FEL

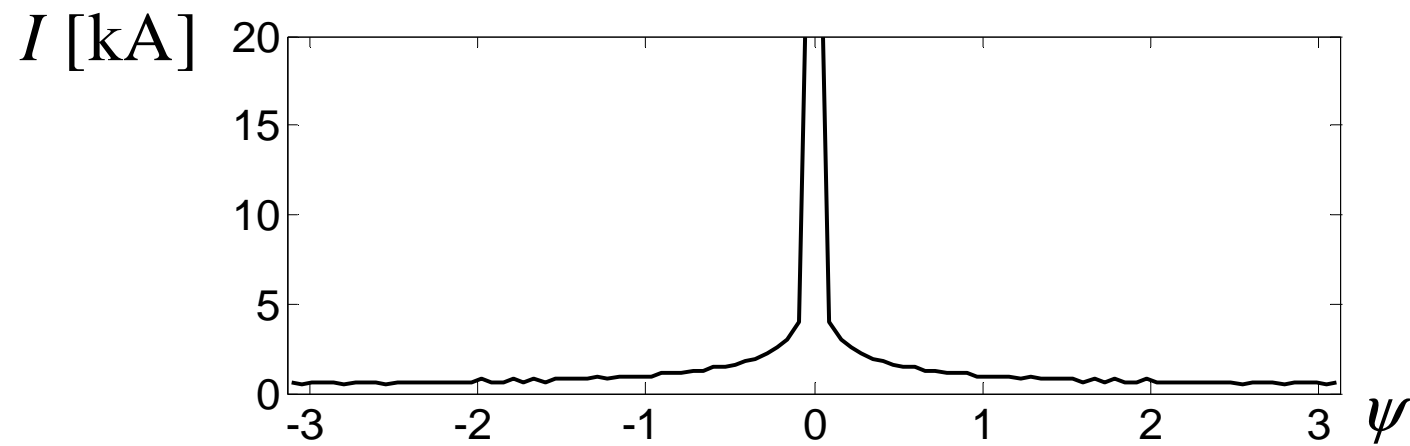
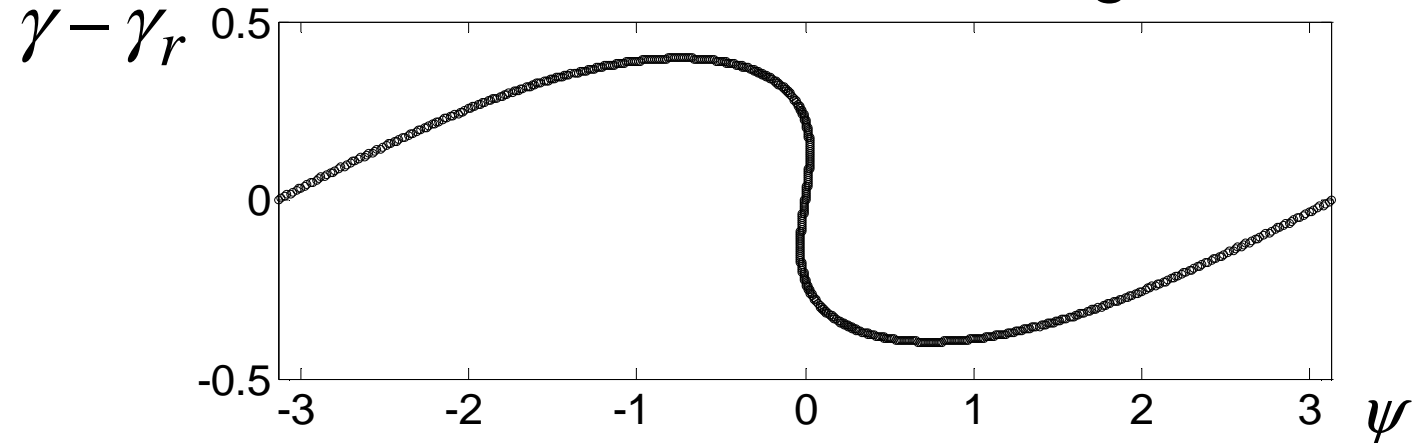
$z = 15\text{m}$



FEL Physics in 1D

„Low gain“ FEL

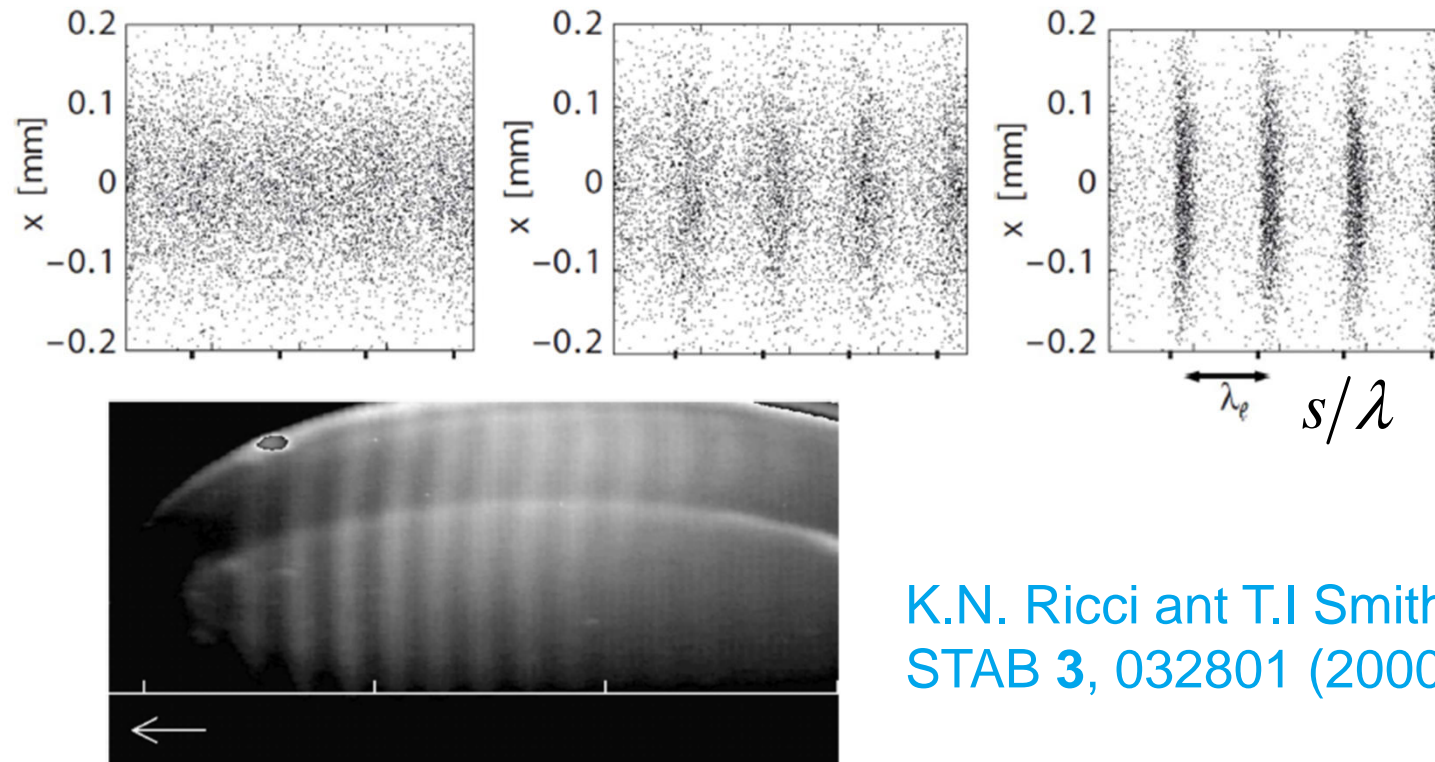
microbunching



FEL Physics in 1D

Microbunching

$$j_z = \Re(\tilde{j}_z) = j_0 + \Re(\tilde{j}_1(z)e^{i\psi})$$

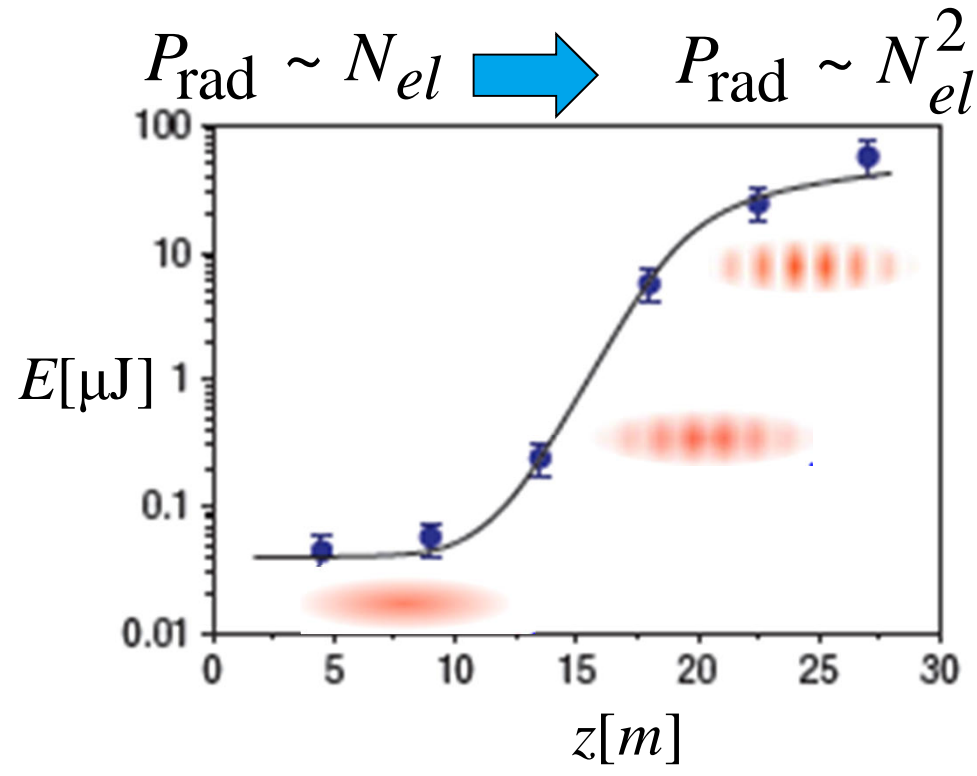


K.N. Ricci ant T.I Smith, PR-STAB 3, 032801 (2000)

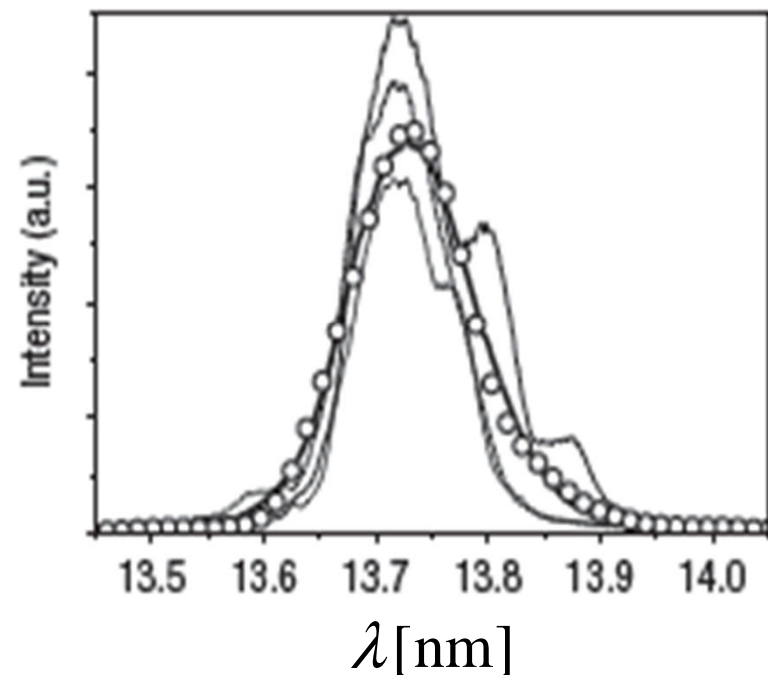
experimental evidence of microbunching in Stanford

FEL Physics in 1D

„High gain“ FEL



experimental data (FLASH)



the amplification
is very high

W. Ackermann et al, Nature Photonics
1, 336 (2007)

FEL Physics in 1D

Field equation

The EM field variation has to be taken into account

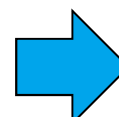
$$\left(\Delta - \frac{1}{c^2} \frac{\partial^2}{\partial t^2} \right) \mathbf{E} = \mu_0 \frac{\partial \mathbf{j}}{\partial t} + \frac{1}{\epsilon_0} \cancel{\nabla \rho} \quad \mathbf{E}(z, t) = \Re(\tilde{\mathbf{E}}(z, t))$$

slowly-varying envelope approximation

$$\tilde{E}_x(z, t) = \tilde{E}_x(z) e^{i(kz - \omega t)} \quad |\tilde{E}_x''(z)| \ll k |\tilde{E}_x'(z)|$$



$$\left[\cancel{\nabla_{\perp}^2} + 2ik \left(\frac{\partial}{\partial z} + \frac{1}{c} \cancel{\frac{\partial}{\partial t}} \right) \right] \tilde{E} = ik \mu_0 c \frac{K}{\gamma} \tilde{j}_1$$



$$\tilde{E}'_x(z) = -\frac{\mu_0 c K}{4\gamma} \tilde{j}_1$$

FEL Physics in 1D

Longitudinal equations of motion

$$\frac{d}{dz} \psi_n = 2k_u \eta_n, \quad n = 1, 2, \dots N$$

$$\frac{d}{dz} \eta_n = -\frac{eK[JJ]}{2m_e c^2 \gamma_r^2} \Re(\tilde{E}_x e^{i\psi_n})$$

Field equation

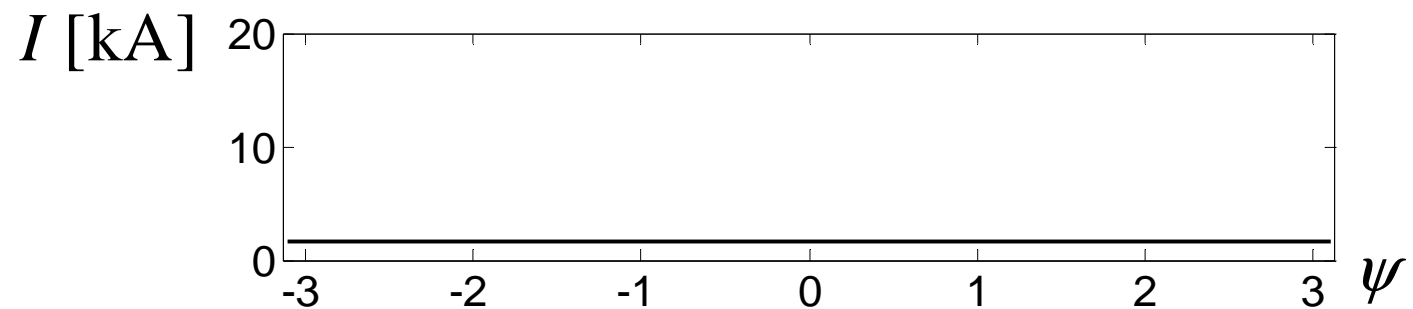
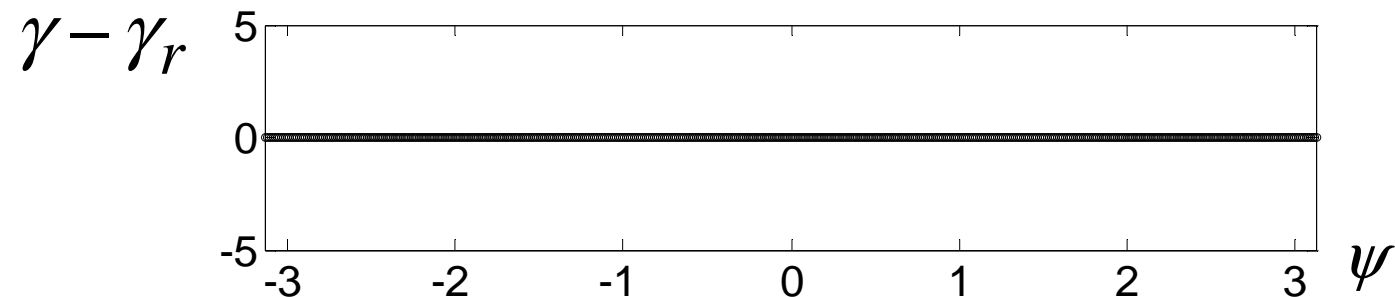
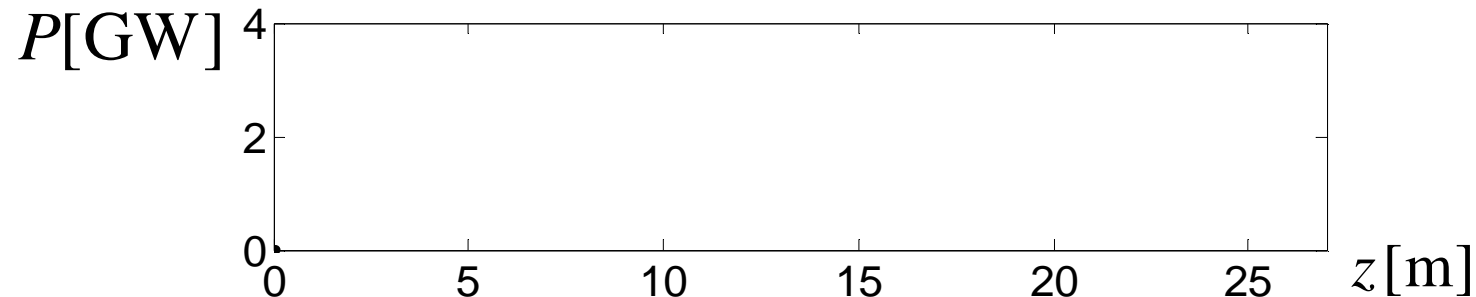
$$\frac{d}{dz} \tilde{E}_x(z) = -\frac{\mu_0 c K}{4\gamma} \tilde{j}_1$$

FEL Physics in 1D

„High gain“ FEL

$$E_x(0) = 0.1 \text{ MV/m}$$

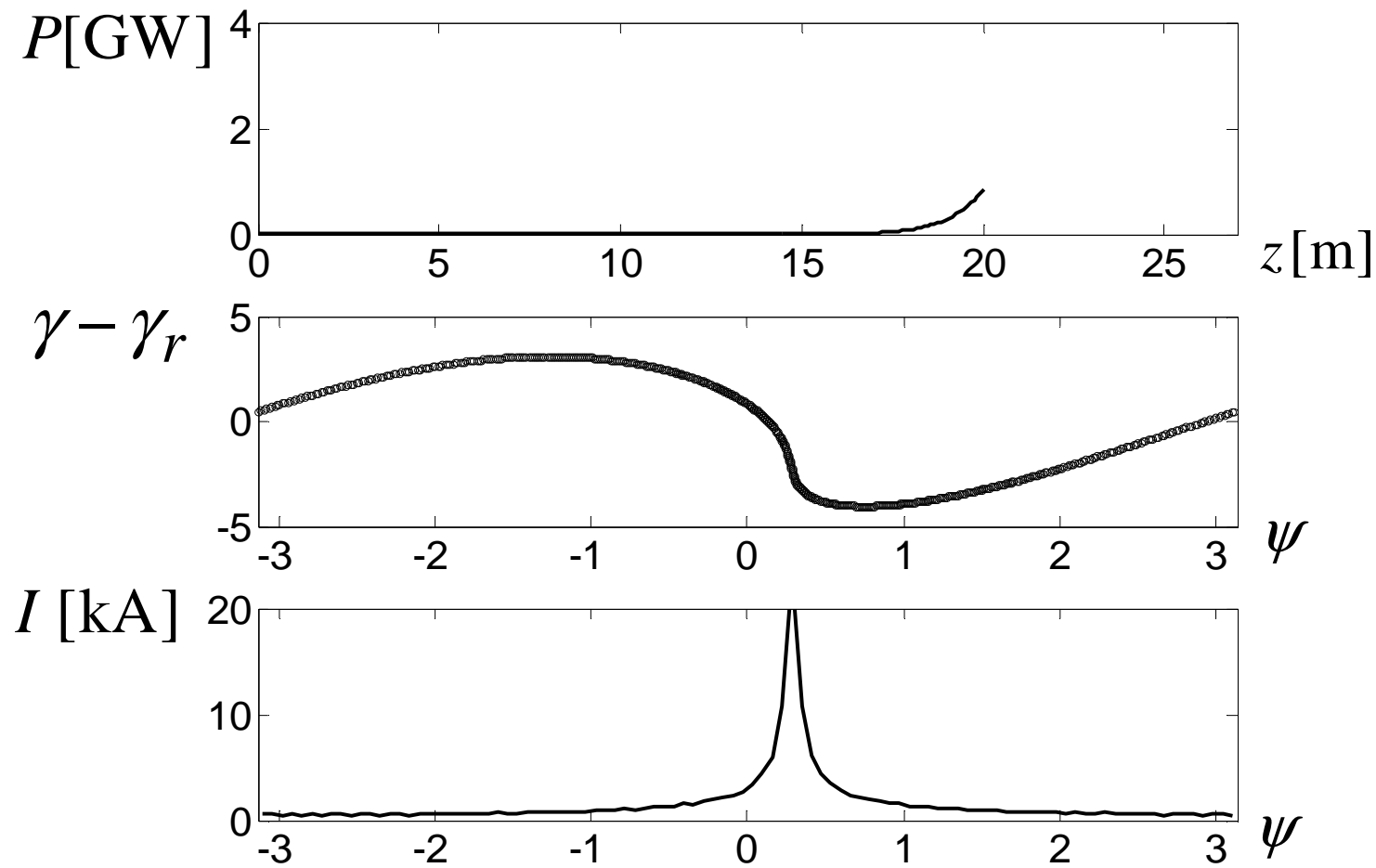
$z = 0 \text{ m}$



FEL Physics in 1D

„High gain“ FEL

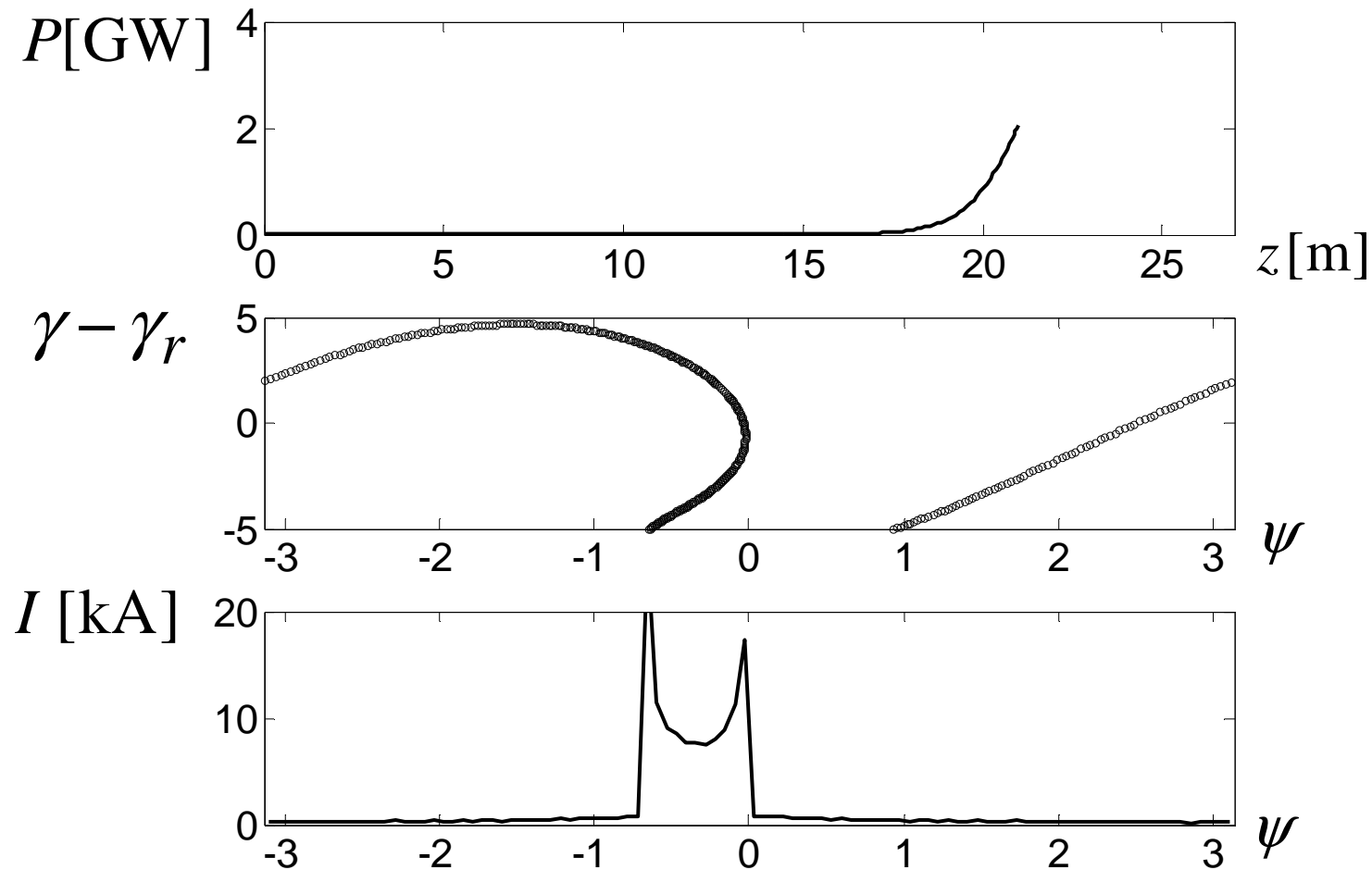
$z = 20\text{m}$



FEL Physics in 1D

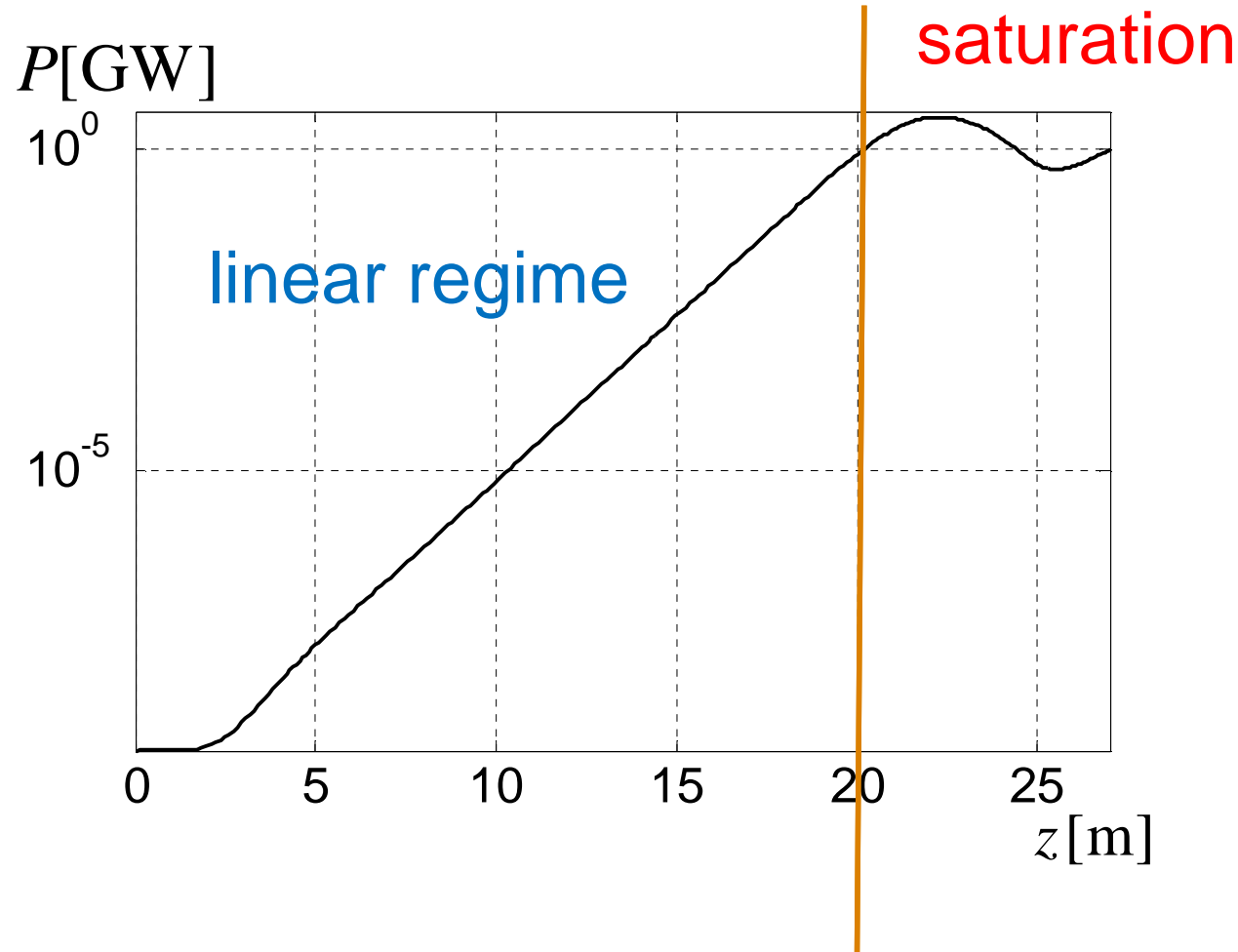
„High gain“ FEL

$z = 21\text{m}$



FEL Physics in 1D

„High gain“ FEL



Mathematical Model in 3D

3D Effekte

- transverse beam dynamics
- space charge effects
- beam properties (emittance, energy spread etc.)
- EM field properties
- undulator properties

FEL codes

FAST
fast

FELEX

FELOS

FELS

FRED3D

RON

GINGER

NUTMEG

SIMPLEX

GENESIS 1.3

ALICE

MEDUSA

PERSEO

SARAH

TDA3D



Numerical Methods

3D FEL codes used at DESY

	FAST (M.Yurkov)	Genesis 1.3 (S.Reiche)	ALICE (I.Zagorodnov)
Equations of motion		Runge-Kutta	leap-frog
EM field	Integral representation	finite-difference, alternating direction	finite difference, Neumann
Boundary conditions	free space	Dirichlet	free space with PML

- the codes are parallelized
- a cluster with 360 processors is used

Mathematical Model in 3D

Equations of motion

$$H^0(\mathbf{r}, \mathbf{p}, t) = c \left(m^2 c^2 + (\mathbf{p} + e\mathbf{A})^2 \right)^{0.5} - e\phi$$

T.M. Tran, J.S.Wurtele,
Review of free-electron-laser (FEL) simulation techniques, Phys. Reports 195 (1990) 1

- change of independent variable

$$H(\mathbf{r}_\perp, ct; \bar{\mathbf{p}}_\perp, \bar{p}_t; z) = -\gamma \left(1 - \frac{1 + |\bar{\mathbf{p}}_\perp|^2 + |\mathbf{a}_\perp|^2 + 2(\bar{\mathbf{p}}_\perp, \mathbf{a}_\perp)}{\gamma^2} \right)^{0.5} + a_z$$

$$\bar{\mathbf{p}}_\perp = \frac{\mathbf{p}_\perp}{mc}$$
$$\mathbf{a} = \mathbf{A} \frac{e}{mc}$$

- **wiggler-period-averaging** (helical undulator)

$$\bar{H}(\mathbf{r}_\perp, ct; \bar{\mathbf{p}}_\perp, \bar{p}_t; z) = -\gamma \left(1 - \frac{1 + |\bar{\mathbf{p}}_\perp|^2 + |\mathbf{a}_\perp|^2}{\gamma^2} \right)^{0.5} + a_z$$

$$a_s \equiv \frac{Ee}{mc\omega}$$

$$|\mathbf{a}_\perp|^2 = K^2 + 2a_s K \sin(\psi + \varphi_s) + a_s^2$$

Mathematical Model in 3D

Equations of motion

longitudinal

$$\frac{d\psi}{dz} = k_w - \frac{1 + |\bar{\mathbf{p}}_\perp|^2 + K^2}{2\gamma^2}$$

transverse (slow)

$$\frac{d \mathbf{r}_\perp}{dz} = \frac{\bar{\mathbf{p}}_\perp}{\gamma \beta_z}$$

$$\frac{d\bar{p}_x}{dz} = - \left(\frac{K^2 k_x^2}{\gamma \beta_z} + \frac{eg}{mc} \right) x$$

$$\frac{d\bar{p}_y}{dz} = - \left(\frac{K^2 k_y^2}{\mathcal{B}_z} - \frac{eg}{mc} \right) y$$



Mathematical Model in 3D

Field equations

- transverse field (*slowly-varying envelope approximation*)

$$E(\vec{r}, t) = \tilde{E}(\vec{r}, t) \exp(i(kz - \omega t)) + c.c. \quad E = E_x + iE_y$$

$$\left[\nabla_{\perp}^2 + 2ik \left(\frac{\partial}{\partial z} + \frac{1}{c} \cancel{\frac{\partial}{\partial t}} \right) \right] \tilde{E} = ik \mu_0 c \frac{K}{\gamma} \tilde{j}_1$$

- longitudinal space charge (on λ scale)

$$\left(\nabla_{\perp}^2 - \frac{n^2(k + k_w)^2}{\gamma_z^2} \right) E_z^{(n)} = \frac{in(k + k_w)}{\epsilon_0 \gamma_z^2} \rho^{(n)}$$

$$E_z(r, \psi) = \sum E_z^{(n)}(r, z) e^{in\psi}$$

Mathematical Model in 3D

Normalized Equations

- equations of motion

$$\frac{d\psi}{d\hat{z}} = \hat{C} + \hat{\eta} - \frac{B}{2} (\hat{x}'^2 + \hat{y}'^2)$$

$$\hat{x}'' = -(\hat{k}_x^2 + \hat{g}) \hat{x}$$

$$\frac{d\hat{\eta}}{d\hat{z}} = |\hat{u}| \cos(\psi + \varphi_s) - \hat{E}_z$$

$$\hat{y}'' = -(\hat{k}_y^2 - \hat{g}) \hat{y}$$

- field equations

$$\left[\frac{1}{2iB} \hat{\Delta}_{\perp} + \frac{d}{d\hat{z}} \right] \hat{u}(\hat{\mathbf{r}}_{\perp}, \hat{z}) = -2a^{(1)}(\hat{\mathbf{r}}_{\perp}, \hat{z})$$

$$\hat{E}_z = \hat{E}_z^{(0)} - \hat{\Lambda}_p^{-2} \frac{1}{N_{jk}} \sum_{i=1}^{N_{jk}} [\pi \operatorname{sgn}(\psi - \psi_i) - (\psi - \psi_i)]$$

Zagorodnov I., Dohlus M., *Numerical FEL studies with a new code ALICE*, FEL09, Liverpool, 2009.

Numerical Methods

Equations of motion

- “leap-frog” scheme for the longitudinal equations

$$\frac{\psi_{j+0.5} - \psi_{j-0.5}}{\Delta z} = \hat{\eta}_j + \hat{C}_j - \frac{B}{2} \left(\hat{x}'_j^2 + \hat{y}'_j^2 \right) \quad j = 1 : N_z$$

$$\frac{\hat{\eta}_{j+1} - \hat{\eta}_j}{\Delta z} = \frac{\hat{u}_{j+1} + \hat{u}_j}{2} \cos \left[\psi_{j+0.5} + \frac{\varphi_{j+1}^s + \varphi_j^s}{2} \right] + \hat{E}_{z,j+0.5},$$

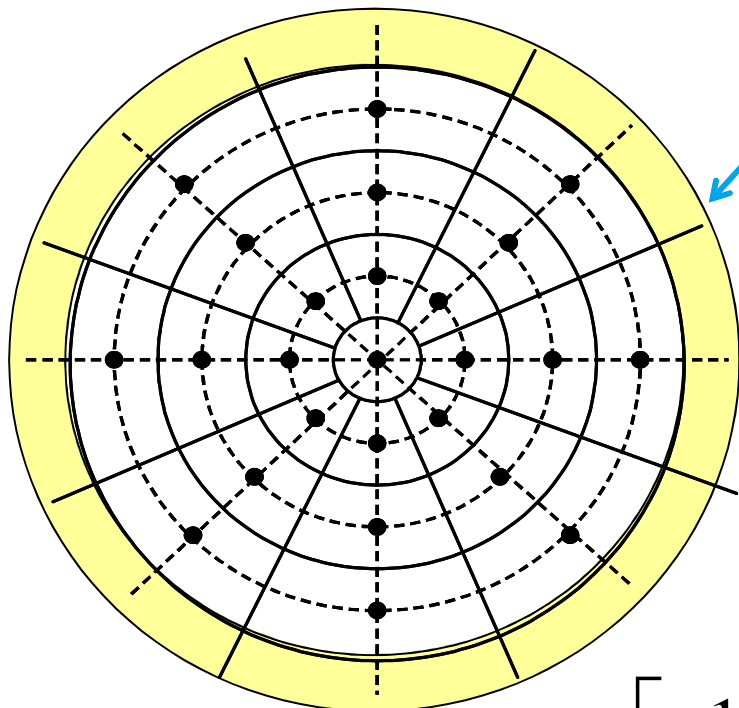
- matrix formalism for the transverse equations

$$\begin{pmatrix} \hat{x}_{j+1} \\ \hat{x}'_{j+1} \end{pmatrix} = M_x \begin{pmatrix} \hat{x}_j \\ \hat{x}'_j \end{pmatrix}$$

$$\begin{pmatrix} \hat{y}_{j+1} \\ \hat{y}'_{j+1} \end{pmatrix} = M_y \begin{pmatrix} \hat{y}_j \\ \hat{y}'_j \end{pmatrix}$$

Numerical Methods

Field equation



Perfectly Matched Layer

F. Collino, Journal of Computational Physics 131, 164 (1997)

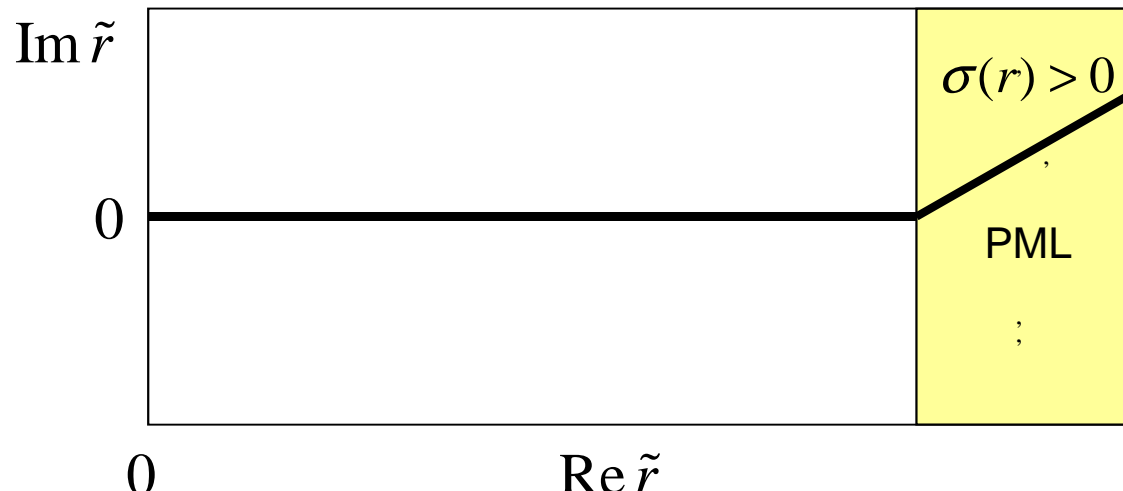
azimuthal expansion

$$\hat{u}(r, z, \phi) = \sum u^{(m)}(r, z) e^{im\phi}$$

$$\left[\frac{1}{2iB} \frac{1}{r} \frac{\partial}{\partial r} r \frac{\partial}{\partial r} - \frac{m^2}{r^2} + \frac{d}{dz} \right] u^{(m)} = -2a^{(1)(m)}$$

Numerical Methods

Perfectly Matched Layer (PML)



$$\tilde{r} = r + \frac{i}{B} \int_0^r \sigma(\xi) d\xi \quad \sigma(r) = \begin{cases} 0, & r \leq r_0 \\ > 0, & r > r_0 \end{cases}$$

- a deformed contour in the complex plane

$$\left[\frac{1}{2iB} \frac{1}{\tilde{r}} \frac{\partial}{\partial \tilde{r}} \tilde{r} \frac{\partial}{\partial \tilde{r}} - \frac{m^2}{\tilde{r}^2} + \frac{d}{dz} \right] u^{(m)} = -2a^{(1)(m)}$$

Numerical Methods

Neumann implicit scheme with PML

$$c_q u_{q+1}^{n+1} + b_q u_q^{n+1} + a_q u_{q-1}^{n+1} = f_q^n$$

The matrix of the system has only three diagonals and we can use the „sweep“ method

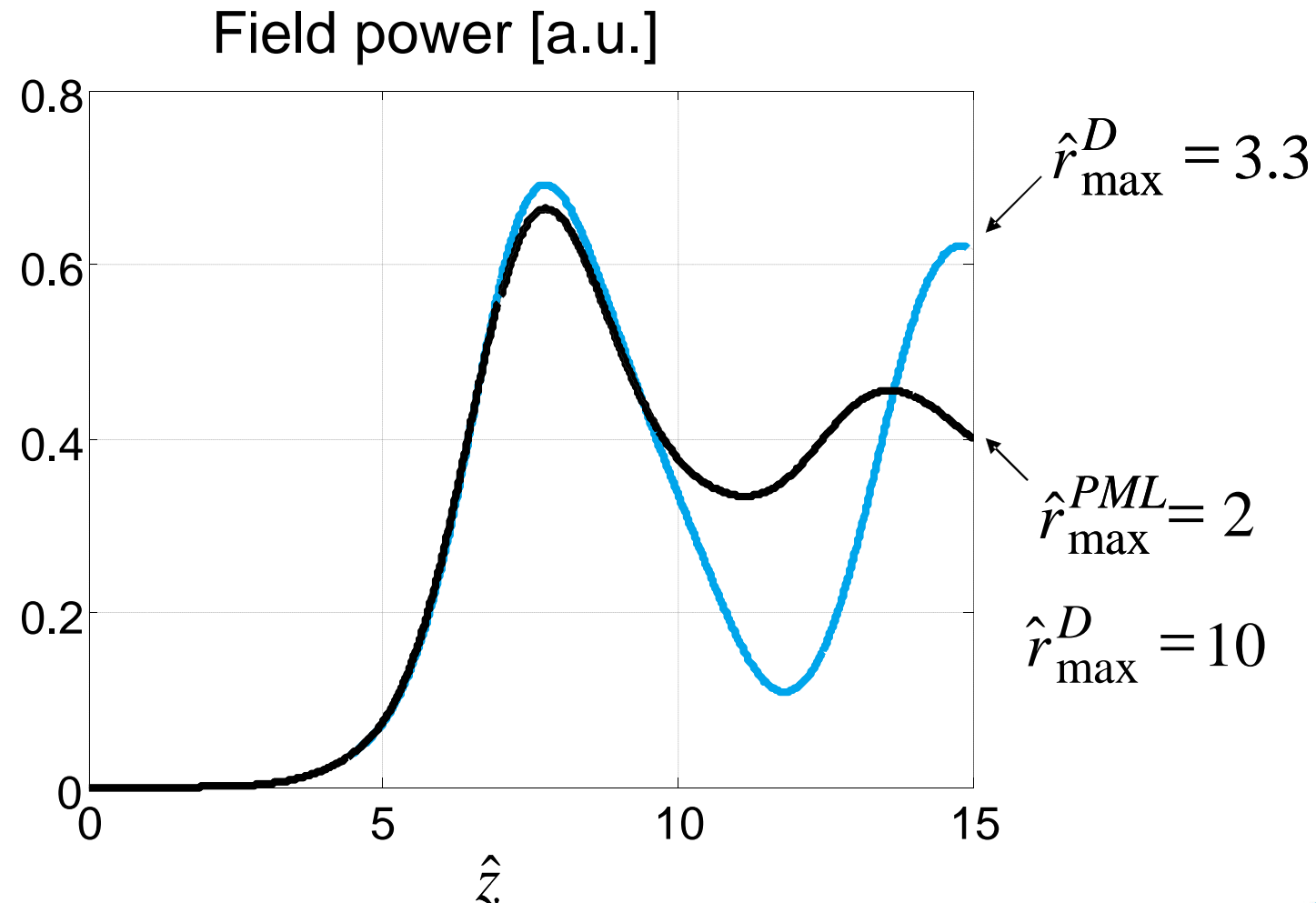
$$a_q = \frac{\Delta z}{4iB} \frac{1}{\tilde{r}_j} \frac{\tilde{r}_{j-0.5}}{(\tilde{r}_{j+0.5} - \tilde{r}_{j-0.5})(\tilde{r}_j - \tilde{r}_{j-1})} \quad b_q = (1 - a_q - c_q) - \frac{\Delta z}{iB} \frac{m^2}{\tilde{r}_j^2}$$

$$c_q = \frac{\Delta z}{4iB} \frac{1}{\tilde{r}_j} \frac{\tilde{r}_{j+0.5}}{(\tilde{r}_{j+0.5} - \tilde{r}_{j-0.5})(\tilde{r}_{j+1} - \tilde{r}_j)}$$

complex numbers!

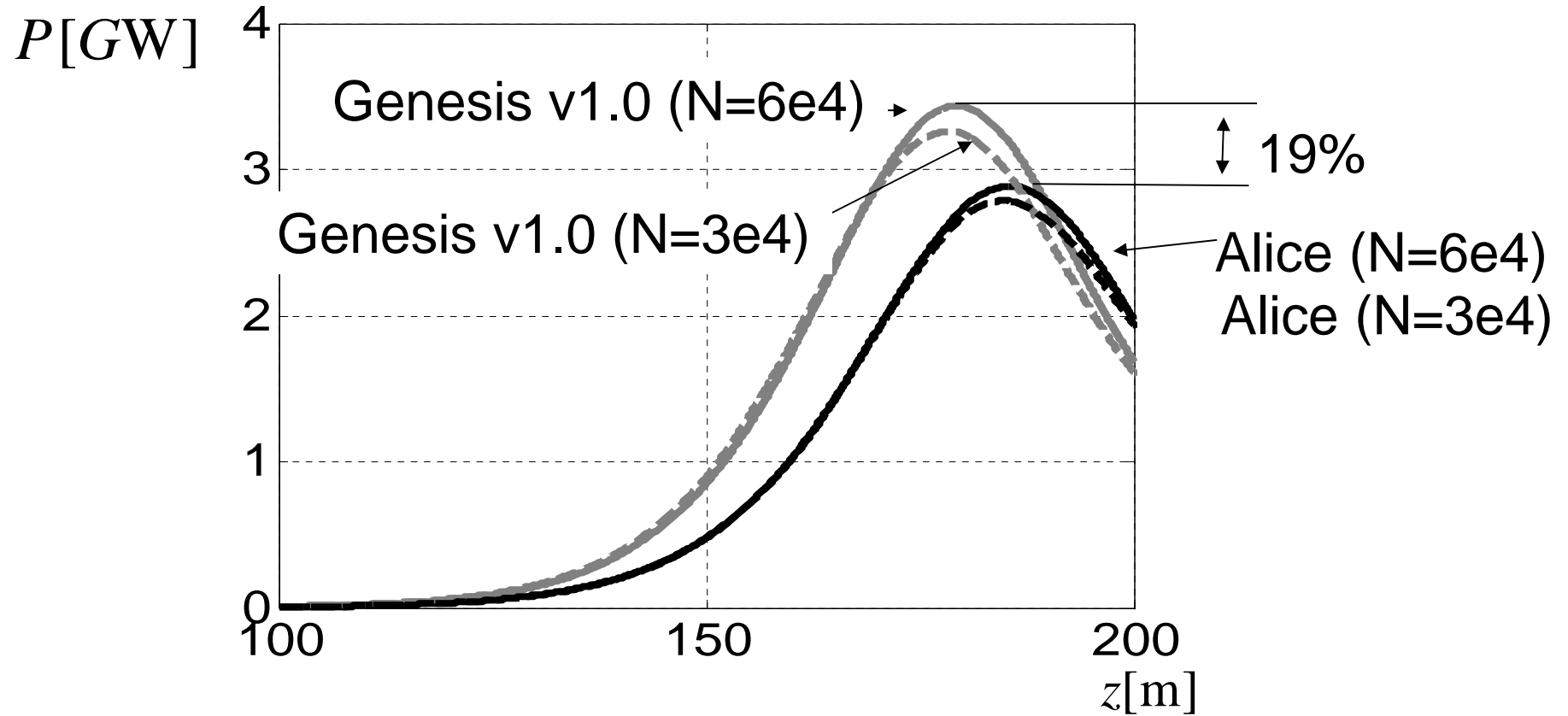
Numerical Methods

PML performance



Quiet Start and Shot Noise

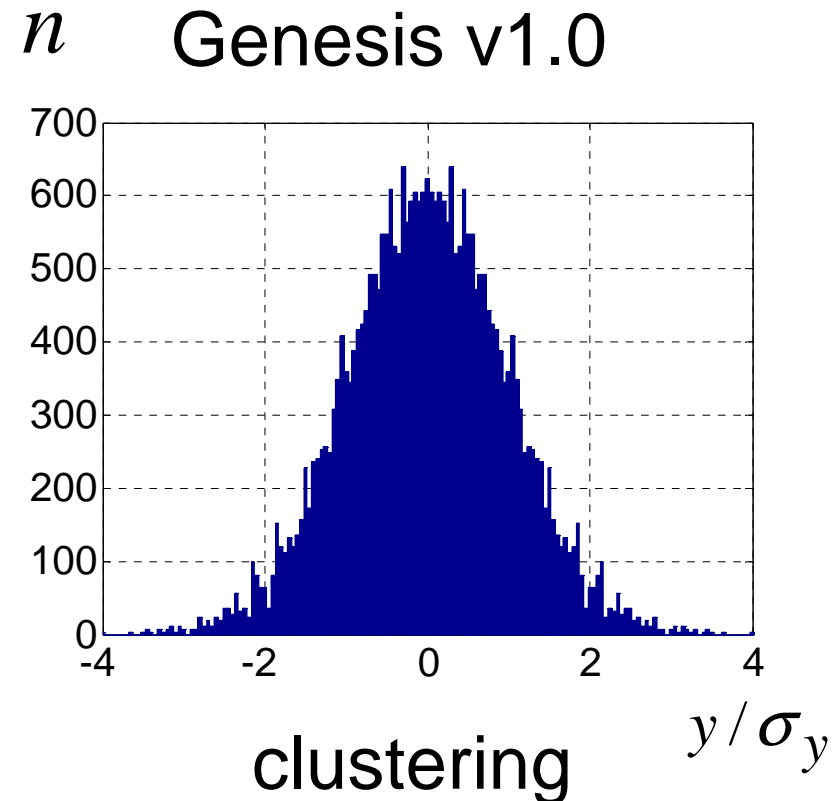
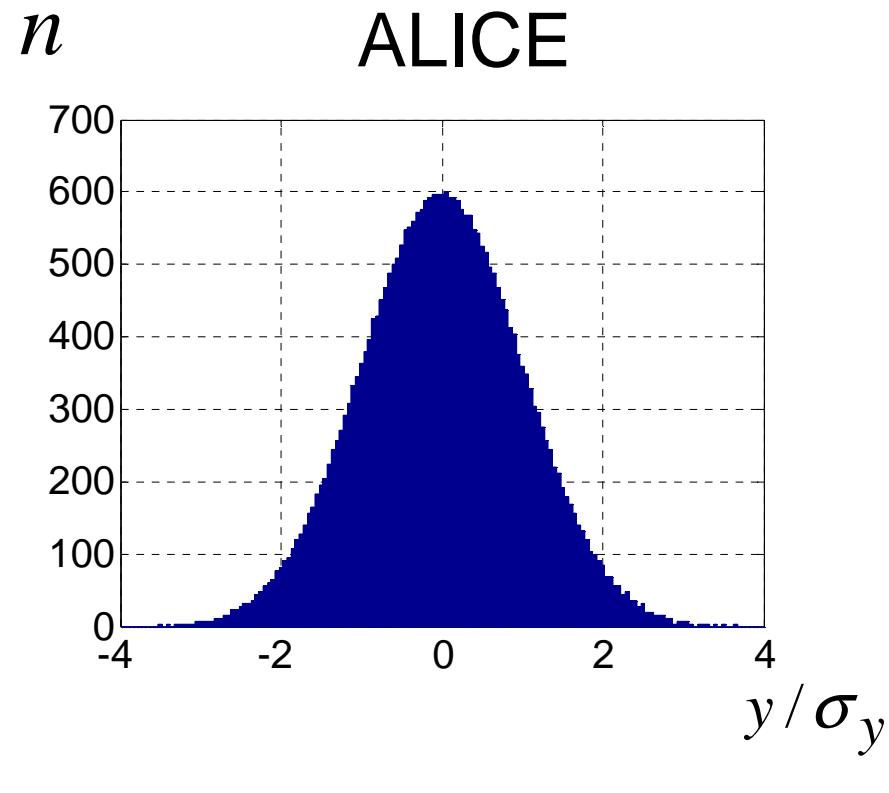
Quiet start in FEL amplifier



The difference in saturation length is 7 %.
The difference in power gain is 19 %.

Quiet Start and Shot Noise

Quiet Start ?



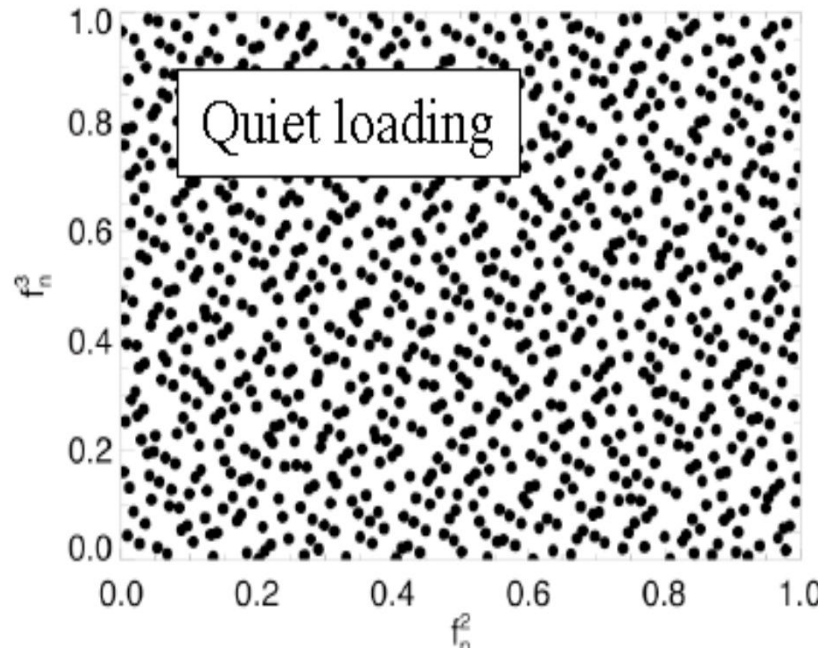
What is the reason?

Quiet Start and Shot Noise

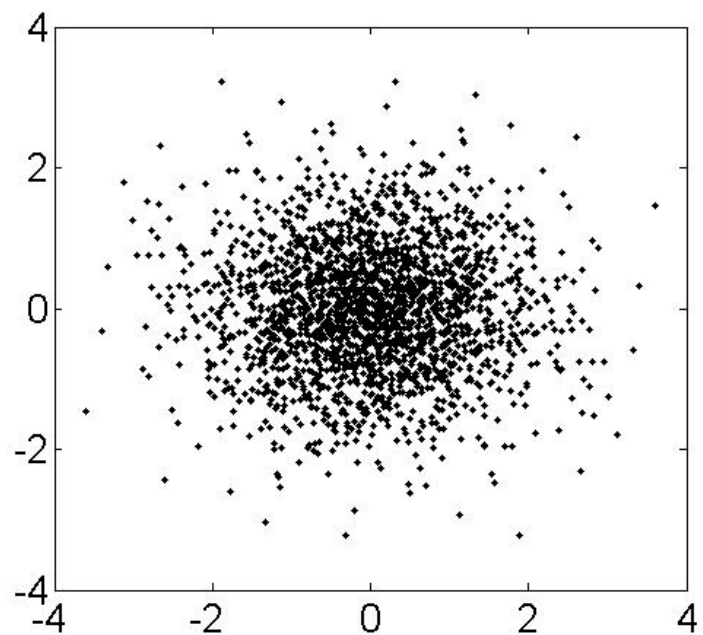
Quiet Start ?

William H. Press et al, Numerical Recipes in Fortran.
The Art of Scientific Computing, 1992

Uniform



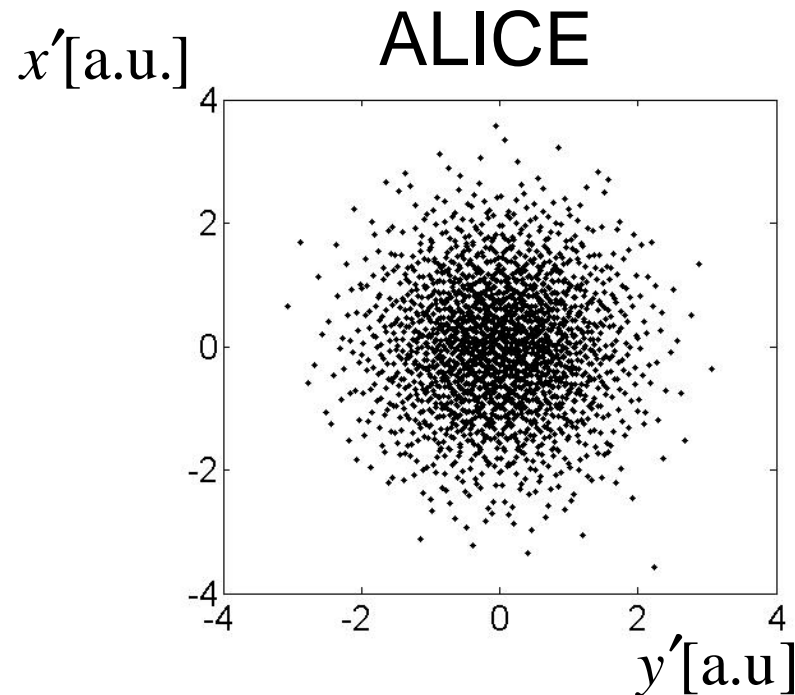
Normal



The polar form of Box-Muller algorithm (in Genesis, ASTRA) maps the „quiet“ uniform distribution in a clustered normal distribution.

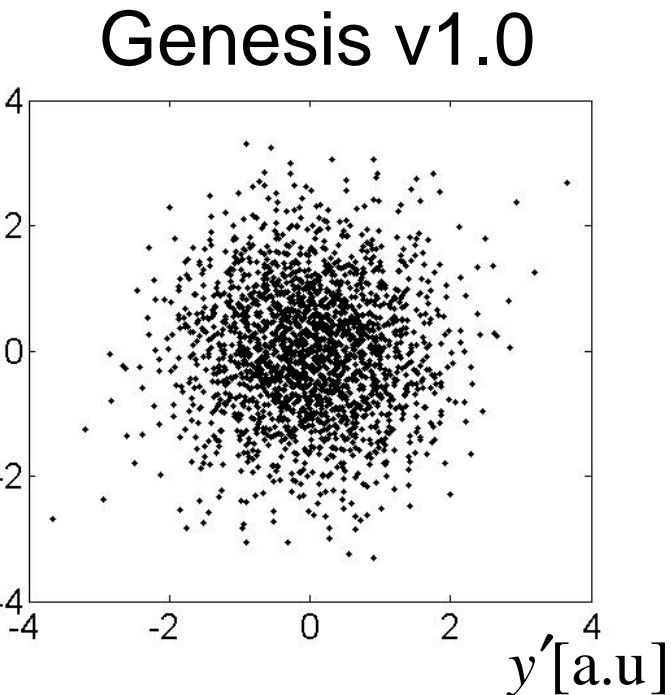
Quiet Start and Shot Noise

Quiet Start ?



inverse error function
transformation

$$Y_i = \sigma \sqrt{2} \operatorname{erf}^{-1}(2X_i - 1) + \mu$$



Box-Mueller algorithm

Quiet Start and Shot Noise

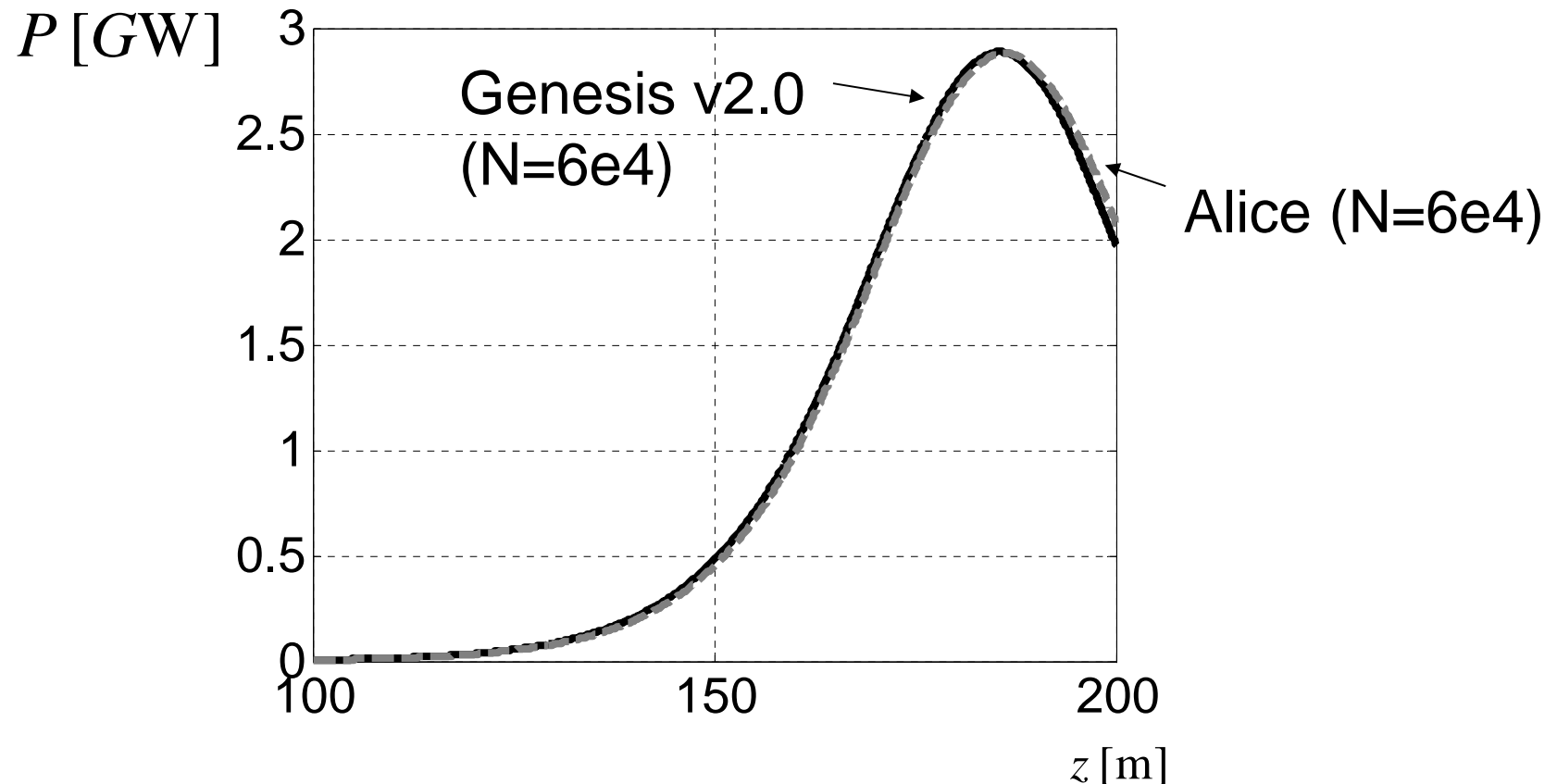
Properties of the normal distribution

$$\delta = \frac{|\sigma_4 - \tilde{\sigma}_4|}{\sigma_4} 100\%$$

	N	δ_x , %	δ_y , %
Genesis v1.0	7500	1.5	7.5
	15000	4.1	4.7
ALICE	7500	0.8	1.0
	15000	0.4	0.4

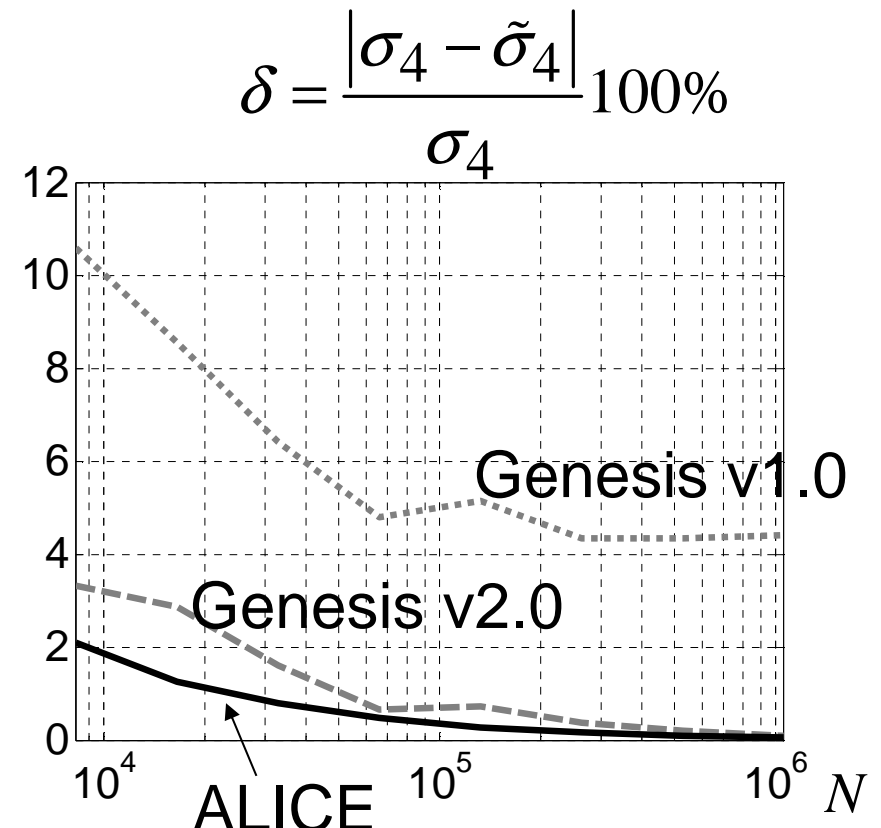
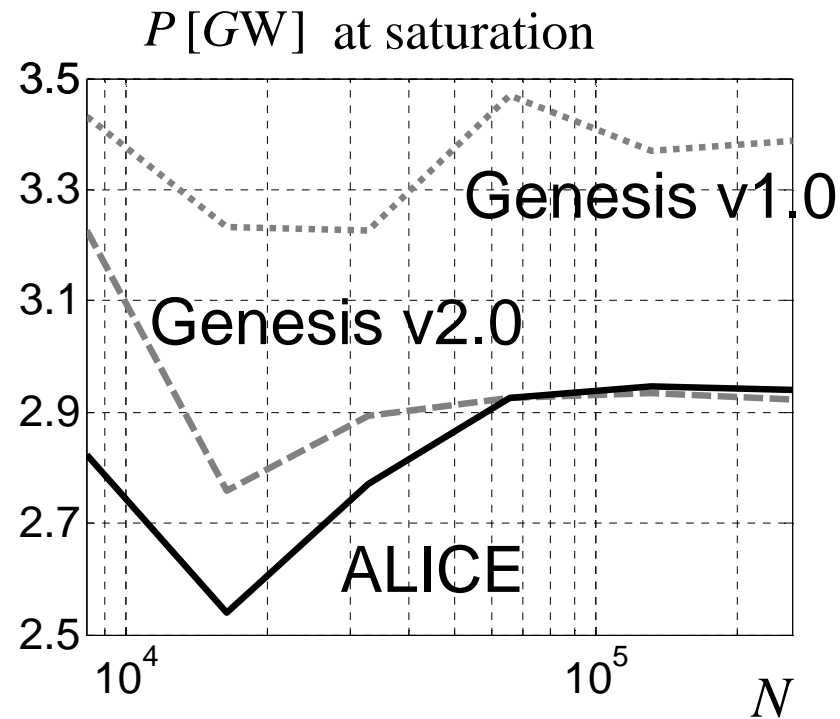
Quiet Start and Shot Noise

New Genesis v2.0 vs. ALICE



Quiet Start and Shot Noise

Convergence



Genesis 1.0:

Hammersley and Box-Mueller

Genesis 2.0:

Hammersley and the inverse error function

ALICE:

Sobol and the inverse error function

Quiet Start and Shot Noise

Shot noise algorithm

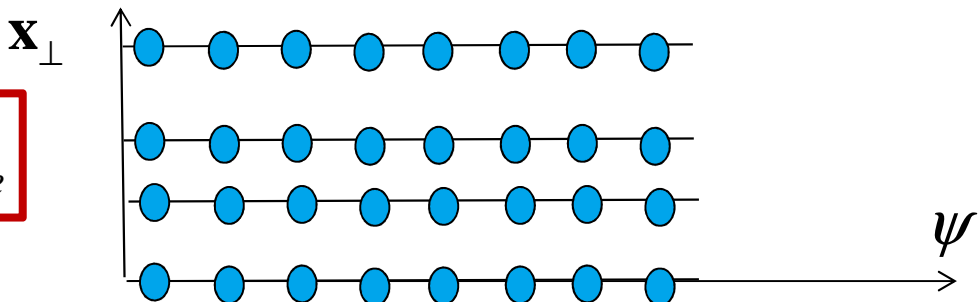
$$b^{(n)} = \frac{1}{N_e} \sum_{m=1}^{N_e} e^{in\psi_m}$$

$$\langle |b^{(n)}| \rangle = \sqrt{\frac{\pi}{4N_e}}$$

$$\langle |b^{(n)}|^2 \rangle = \frac{1}{N_e}$$

- beamlets and variation in position (W.Fawley)
- variations in charges (B.McNeil et al.)

$$N \ll N_e$$



beamlets - a set of $2M$ particles with the same position $\mathbf{x}_\perp = (x, y, p_x, p_y, \gamma)$

N_b beamlets with $2M$ particles each.

$$\langle |b_k^{(j)}|^2 \rangle = 0; \quad k = 1:N_b, j = 1:M$$

Quiet Start and Shot Noise

Shot noise algorithm

Small position variations

W.M. Fawley, Phys. Rev. STAB 5 (2002) 070701

$$\delta\theta_j = \sum_{m=1}^{m=M} a_m \cos(m\theta_j) + b_m \sin(m\theta_j) \quad j = 1 : 2M$$

$$a_{m,rms} = b_{m,rms} = \sqrt{\frac{2}{N_b m^2}}, \quad m \leq M ?!$$

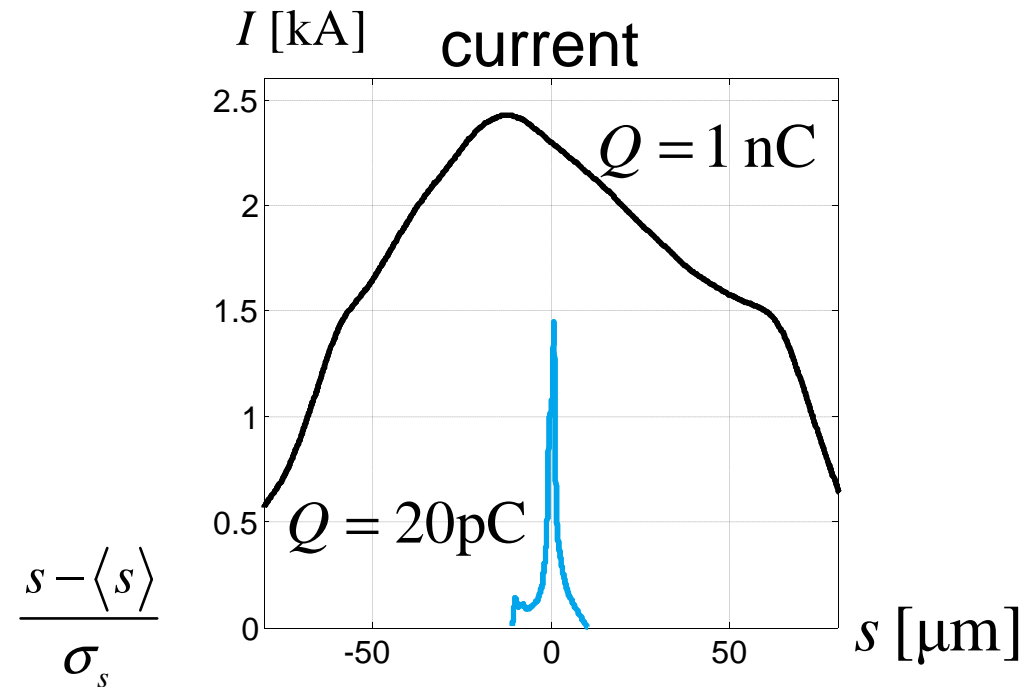
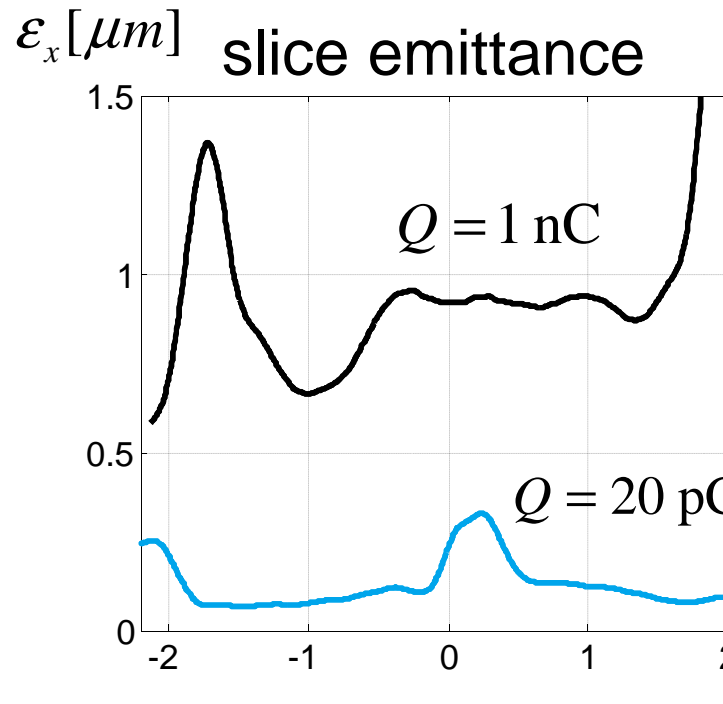
A more careful analysis for the highest harmonic $m=M$ yields

$$a_{M,rms} = b_{M,rms} = \sqrt{\frac{1}{N_b M^2}}$$

Time Dependent Simulations

Slice parameters are extracted from
“Gun-to-Undulator” simulations

γ $\Delta\gamma$ ε_x ε_y β_x β_y $\langle x \rangle$ $\langle y \rangle$ $\langle x' \rangle$ $\langle y' \rangle$ α_x α_y I



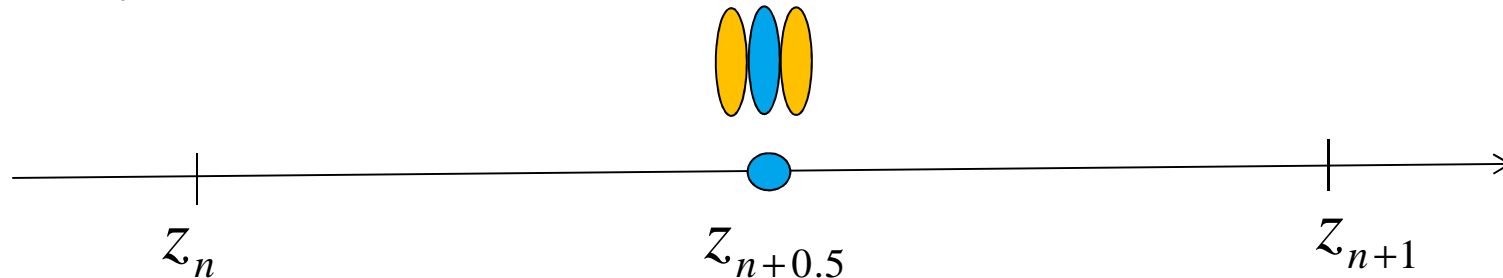
Time Dependent Simulations

Field equation

$$\left[\nabla_{\perp}^2 + 2ik \left(\frac{\partial}{\partial z} + \frac{1}{c} \frac{\partial}{\partial t} \right) \right] \tilde{E}(z, t) = ik \mu_0 c \frac{K}{\gamma} \tilde{j}_1(z, t)$$

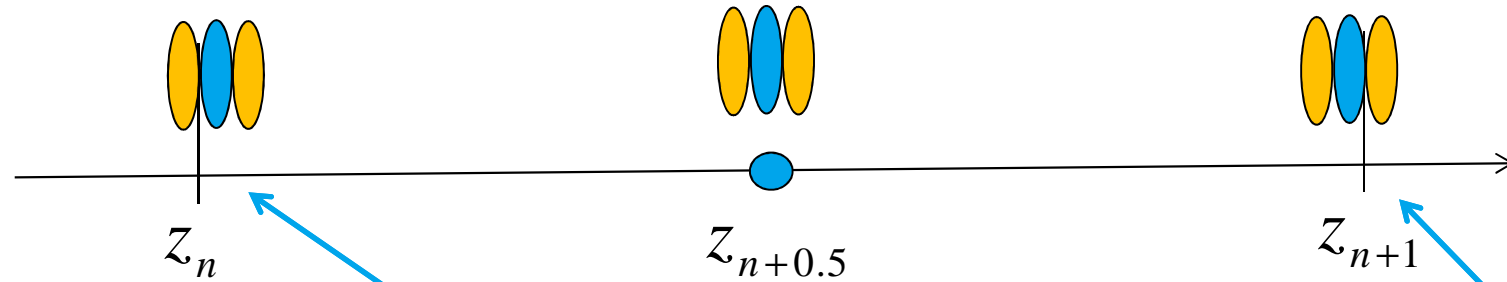
$$t = t_0 + \frac{z}{c} \quad \longrightarrow \quad \left[\frac{\nabla_{\perp}^2}{2ik} + \frac{d}{dz} \right] \tilde{E}\left(z, t_0 + \frac{z}{c}\right) = F\left(z, t_0 + \frac{z}{c}\right)$$

$t_j(z_{n+0.5})$ - the time when slice j reaches position $z_{n+0.5}$



$$\frac{d}{dz} \tilde{E}(z_{n+0.5}, t_j(z_{n+0.5})) = \frac{\tilde{E}\left(z_{n+1}, t_j(z_{n+0.5}) + \frac{0.5\Delta z}{c}\right) - \tilde{E}\left(z_n, t_j(z_{n+0.5}) - \frac{0.5\Delta z}{c}\right)}{\Delta z} + O(2)$$

Time Dependent Simulations



$$t_j(z_{n+0.5}) - \frac{0.5\Delta z}{c} = t_{j-0.5}(z_n)$$

$$t_j(z_{n+0.5}) + \frac{0.5\Delta z}{c} = t_{j+0.5}(z_{n+1})$$

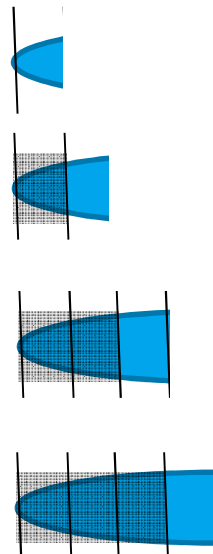
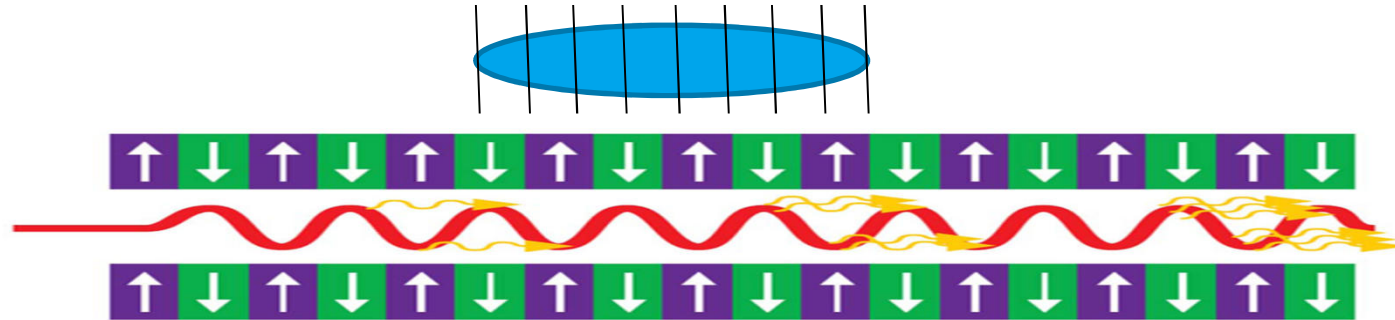
field of the current slice j

$$\frac{\nabla_\perp^2}{2ik} \left(\frac{\tilde{E}_{n+1}^j + \tilde{E}_n^{j-1}}{2} \right) + \frac{\tilde{E}_{n+1}^j - \tilde{E}_n^{j-1}}{\Delta z} = F(z_{n+0.5}, t_j(z_{n+0.5}))$$

$$\tilde{E}_n^j = \tilde{E}(z_n, t_{j+0.5}(z_n))$$

Time Dependent Simulations

Parallel algorithm

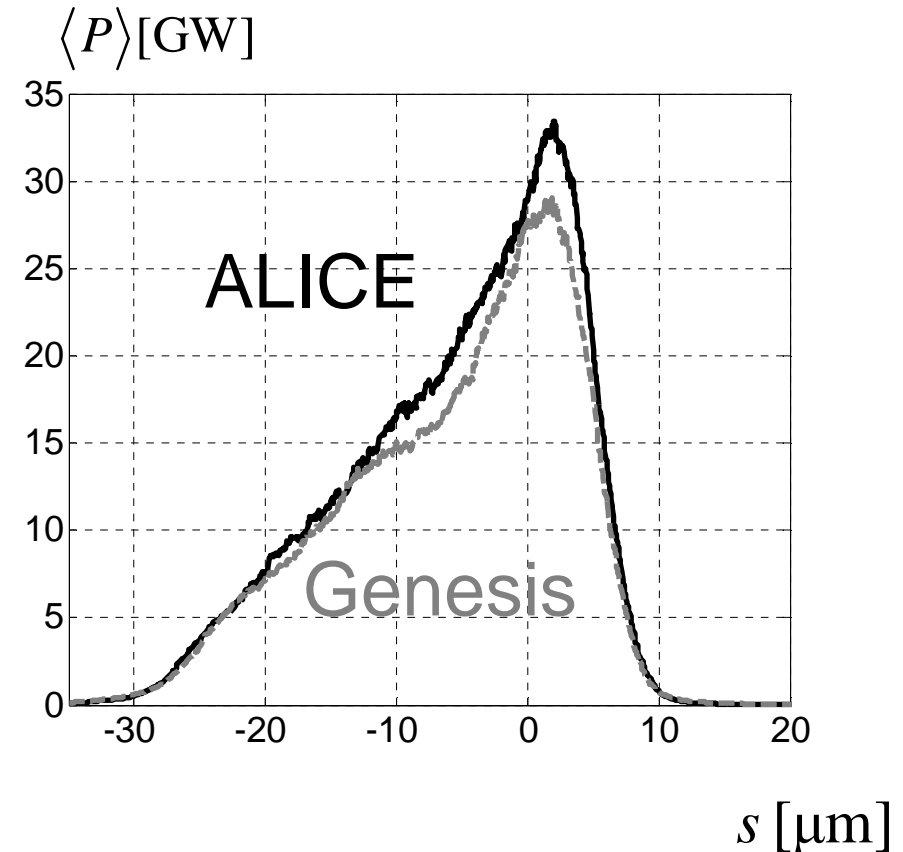
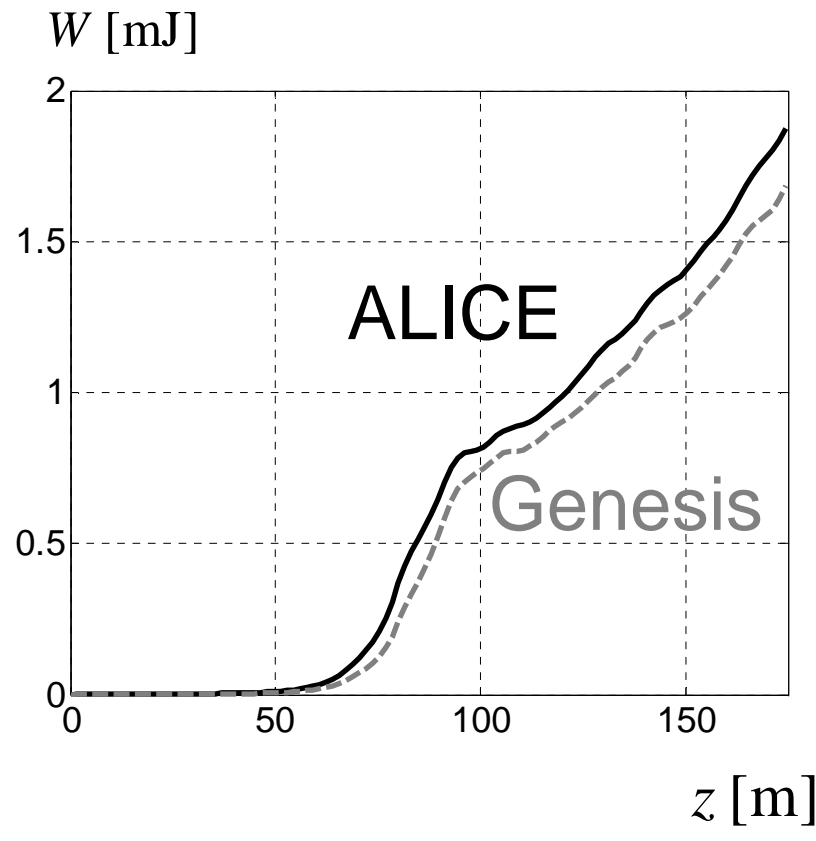


„Slice for slice“

- we start from the last slice and track the particles of this slice through the undulator; the radiated EM field is saved.
- then we track the next slice in the radiation field of the previous slices

Time Dependent Simulations

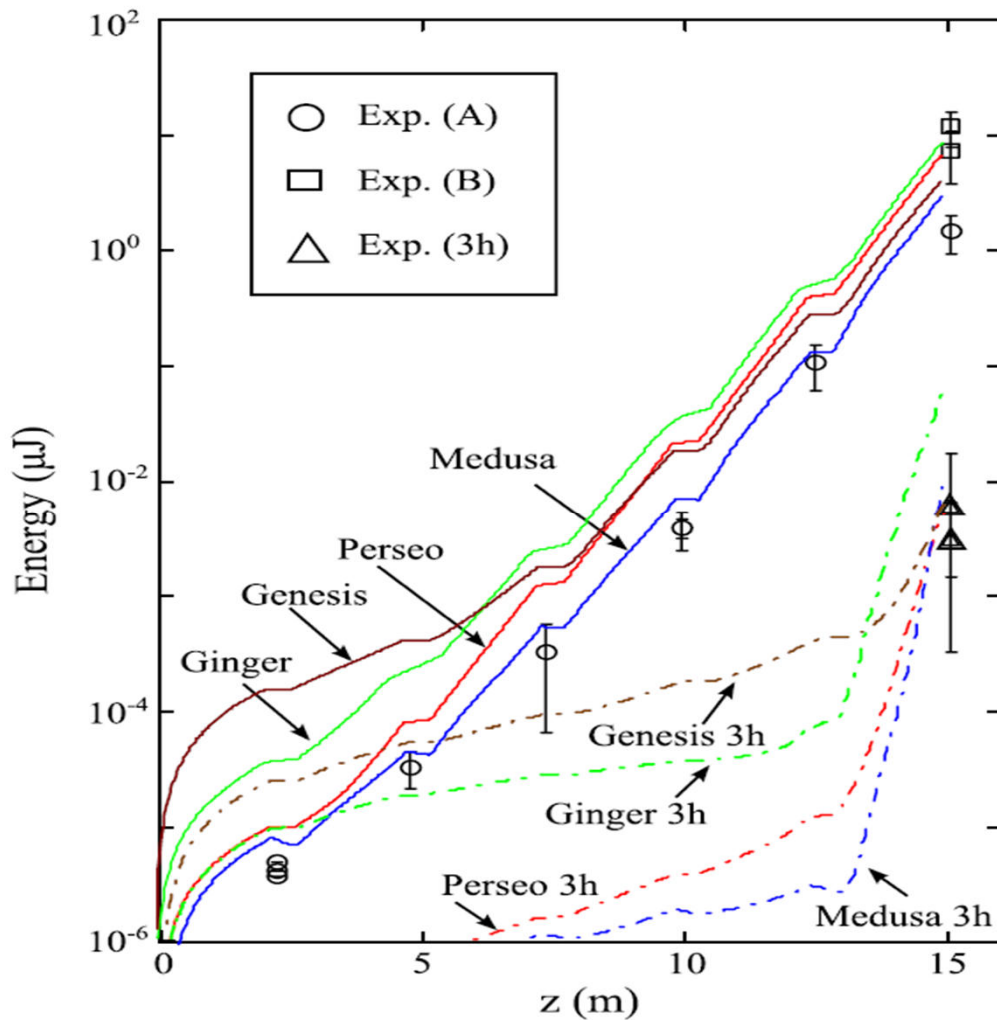
SASE in the European XFEL



I.Zagorodnov, Ultra-short low charge operation at FLASH and the European XFEL, FEL 2010, Malmö, 2010

Problems and Challenges

Comparison with SPARC FEL experiment



L. Giannesi et al, PR STAB 14, 060712(2011)

Medusa is a code based on non-averaged equations

Problems and Challenges

Limitations of the considered FEL model

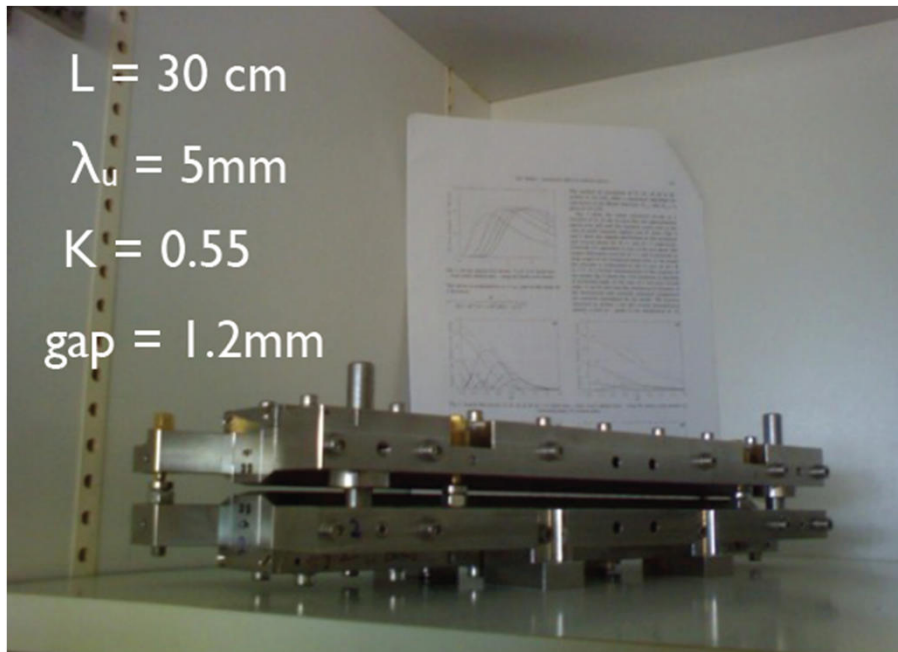
- fast „slalom“ motion is not modeled
- only forward propagating field is considered
- macroparticles are locked in the slice with periodic boundary conditions
- only low order harmonics are simulated correctly
- macroscopic space charge, bunch shape changes are not modeled
- narrow frequency bandwidth near the resonance frequency, narrow energy spread



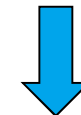
Problems and Challenges

“Table-Top-FEL”

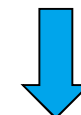
M.Fuchs et al, Nature Physics 5, 826(2009)



strong space charges,
large energy spread



fast bunch shape change



- charge or macroparticles redistribution
- macroscopic space charge equation
- non-averaged modell

Summary

- FEL codes based on averaged equations are checked by experiments
- new FEL schemes (Table Top FEL, Echo-Enabled High-Harmonic Generation etc.) require to consider more physics
- FEL codes based on non-averaged FEL equations, with macroscopic space charge are under development

H.P. Freund, S.G. Biedron, S.V. Milton, IEEE J.
Quantum Electron. 36 (2000) 275. (Medusa code)

C.K.W. Nam, P. Aitken, and B.W.J. McNeil, Unaveraged three-dimensional modelling of the FEL, FEL 2008, Gyeongju, Korea, 2008

